TKK Dissertations 45
Espoo 2006

TRANSIENT PERFORMANCE ANALYSIS OF WIND-POWER INDUCTION GENERATORS

Doctoral Dissertation

Slavomir Seman

Helsinki University of Technology
Department of Electrical and Communications Engineering
Laboratory of Electromechanics

TKK Dissertations 45
Espoo 2006

TRANSIENT PERFORMANCE ANALYSIS OF WIND-POWER INDUCTION GENERATORS

Doctoral Dissertation

Slavomir Seman

Dissertation for the degree of Doctor of Science in Technology to be presented with due permission of the Department of Electrical and Communications Engineering for public examination and debate in Auditorium S1 at Helsinki University of Technology (Espoo, Finland) on the 10th of November, 2006, at 12 noon.

Helsinki University of Technology
Department of Electrical and Communications Engineering
Laboratory of Electromechanics

Teknillinen korkeakoulu
Sähkö- ja tietoliikennetekniikan osasto
Sähkömekaniikan laboratorio

Distribution:
Helsinki University of Technology
Department of Electrical and Communications Engineering
Laboratory of Electromechanics
P.O. Box 3000
FI - 02015 TKK
FINLAND
URL: http://sahko.tkk.fi/
Tel. +358-9-4511
E-mail: electromechanics@hut.fi

ISBN-13 978-951-22-8422-1
ISBN-10 951-22-8422-7
ISBN-13 978-951-22-8423-8 (PDF)
ISBN-10 951-22-8423-5 (PDF)
ISSN 1795-2239
ISSN 1795-4584 (PDF)
URL: http://lib.tkk.fi/Diss/2006/isbn9512284235/

TKK-DISS-2193

Picaset Oy
Helsinki 2006

HELSINKI UNIVERSITY OF TECHNOLOGY
P. O. BOX 1000, FI-02015 TKK
http://www.tkk.fi

ABSTRACT OF DOCTORAL DISSERTATION

Author Slavomir Seman

Name of the dissertation

Transient performance analysis of wind-power induction generators

Date of manuscript 12.05.2006 | Date of the dissertation 10.11.2006

☐ Monograph | ☒ Article dissertation (summary + original articles)

Department Electrical and Communications Engineering
Laboratory Laboratory of Electromechanics
Field of research Electromechanics, Electric Drives
Opponent(s) Prof. J. Pyrhönen
Supervisor Prof. A. Arkkio
(Instructor)

Abstract

A coupled field-circuit simulator for the transient analysis of wind energy conversion systems with a doubly fed induction generator (DFIG) was developed and experimentally validated. Short-term grid disturbance and ride-through analyses were carried out for a 1.7-MW DFIG wind-power conversion system. Two simulation models of the wind-power DFIG were compared to reveal the consequences of the different modeling approaches for the accuracy of transient analysis. The DFIG was represented in the simulator by an analytical two-axis model with constant lumped parameters or by a finite element method-based model. The model of the generator was coupled with a model of the crowbar-protected and direct torque-controlled frequency converter, a model of the main transformer, and a simple model of the grid. In addition, a detailed model of the wind turbine was compared with a simplified model that omits the model of the mechanical part of the wind turbine. The simulator was experimentally validated by a 1.7-MW full-scale measurement set-up. The comparison between the simulated and measured results shows reasonable agreement. The analytical model of the DFIG, however, manifests certain drawbacks that are overcome by using a FEM model. The developed coupled field circuit-based simulator has proved to be capable and reliable for modeling of complicated power electronics and electrical machine set-ups and thus is a useful tool for the development and optimization of wind-power generators.

Keywords coupled simulator, crowbar, doubly fed induction generator, transient analysis, ride-through, wind turbine

ISBN (printed) 951-22-8422-7 | ISSN (printed) 1795-2239

ISBN (pdf) 951-22-8423-5 | ISSN (pdf) 1795-4584

ISBN (others) | Number of pages 112

Publisher Helsinki University of Technology, Laboratory of Electromechanics

Print distribution Helsinki University of Technology, Laboratory of Electromechanics

☒ The dissertation can be read at http://lib.tkk.fi/Diss/2006/isbn9512284235

Preface

The research was carried out in the Laboratory of Electromechanics at Helsinki University of Technology. The work is a part of a research project about the coupling of the finite element solver with a system simulator that was used as the main tool for carrying out the simulation analysis presented in this thesis. The work was financed by the National Technology Agency of Finland (Tekes), ABB Oy, Fortum Power and Heat Oy, and the Laboratory of Electromechanics.

I would like to express my gratitude to Emeritus Professor Tapani Jokinen, who offered me an opportunity to work in the Laboratory of Electromechanics and guided me at the beginning of my doctoral studies. I am obliged to my supervisor, Professor Antero Arkkio, for his guidance, advice, and generous help, as well as to the head of the laboratory, Professor Asko Nimenmaa, for his encouragement and support during the course of this work.

I owe a great debt of appreciation to Dr. Jouko Niiranen from ABB Oy for the generous help he has given to me in scientific and practical matters, for invaluable discussions, and measured data provision. I would like to thank Dr. Sami Kanerva for his remarkable contribution to this work by developing the coupled simulator and helping in the development of the simulation models, as well as for his valuable comments and suggestions. I also wish to thank Dr. Florin Iov from the Institute of Energy Technology of Aalborg University for his contribution to this work and help in the modeling of variable-speed wind turbines and to all my colleagues at the Laboratory of Electromechanics for their kindness and the help they have provided to me during the work.

Consultations with Dr. Julius Saitz from the Laboratory of Electromechanics, Dr. Aron Szucs, and Reijo Virtanen from ABB Oy are gratefully acknowledged.

The additional financial support given by Tekniikan edistämissäätiö, the Fortum Foundation, and the Research Foundation of Helsinki University of Technology is gratefully acknowledged.

Last but not least, my thankful thoughts go to my parents for their encouragement, to my beloved wife, Marianna, for her patience and great support during this work and to my two sons, Samuel and Jakub, for their smiles, which bring a lot of happiness into my life, and therefore I dedicate this work to them.

Espoo August 2006

Slavomir Seman

List of publications

P1 Seman, S., Niiranen, J., Kanerva, S., Arkkio, A. 2004. "Analysis of a 1.7 MVA Doubly Fed Wind-Power Induction Generator during Power Systems Disturbances". *Proceedings of NORPIE 2004*, 14-16 June 2004, Trondheim, Norway, 6 p., (CD-ROM), Available:http://www.elkraft.ntnu.no/norpie/10956873/Final%20Papers/046%20-%20 NORP-Seman.pdf (7.5.2006).

P2 Seman, S., Kanerva, S., Niiranen, J., Arkkio, A. 2004. "Transient Analysis of Wind Power Doubly Fed Induction Generator Using Coupled Field Circuit Model", *Proceedings of ICEM 2004*, 5-8 September 2004, Cracow, Poland, 6 p., (CD-ROM).

P3 Kanerva, S., Seman, S., Arkkio, A. 2005. "Inductance Model for Coupling Finite Element Analysis with Circuit Simulation", *IEEE Transaction on Magnetics*, Vol. 41, Issue 5, May 2005, pp. 1620-1623.

P4 Seman, S., Niiranen, J., Kanerva, S., Arkkio, A., Saitz, J. 2005. "Performance Study of Doubly Fed Wind-Power Generator under Network Disturbances", *IEEE Transaction on Energy Conversion*, Accepted for future publication, Available: http://ieeexplore.ieee.org/iel5/60/26781/101109TEC2005853741.pdf?tp=&arnumber=101109TEC2005853741&isnumber=26781, 8 p., (7.5.2006).

P5 Seman, S., Iov, F., Niiranen, J., Arkkio, A. 2005. "Comparison of Simulators for Variable Speed Wind Turbine Transient Analysis", *International Journal of Energy Research*, Vol. 30, Issue 9, pp. 713-728, Available: http://www3.interscience.wiley.com/cgi-bin/fulltext/112579563/PDFSTART, 16 p., (7.5.2006).

P6 Seman, S., Niiranen, J., Arkkio, A. 2006. "Ride-Through Analysis of Doubly Fed Induction Wind-Power Generator under Unsymmetrical Network Disturbance", *IEEE Transaction on Power Systems*, 7 p., Accepted for future publication.

Contents

List of symbols

A = magnetic vector potential

A_k^{ave} = average vector potential on the coil side

$\boldsymbol{B}$ = magnetic flux density

C_p = power coefficient

C_{stray} = stray capacitance of the transformer winding

D_{amp} = equivalent damping factor

f_N = rated stator frequency

f_{sw} = optimal switching frequency

$\boldsymbol{H}$ = magnetic field strength

I_{crow} = current flowing via crowbar resistor

I_{net} = dc current flowing between dc link and network side

I_{rot} = dc current flowing between dc link and rotor-side converter

$\underline{i}_s$, $\underline{i}_r$, $\underline{i}_m$ = space vector of the stator, rotor, and magnetizing current

i_{rx} , i_{ry} = rotor current components in the two-axis rotational reference frame

i_w = phase current

J, J_{gen} = induction generator moment of inertia

J_{wtr} = wind turbine moment of inertia

$J_{wheel\ 1,2}$ = gearbox wheel moment of inertia

K_{gear} = gearbox ratio

K_{PI} = proportional gain

K_{stiff} = equivalent stiffness factor

l_k = length of the coil side

l_e = axial length

L_e = additional end-winding inductance

L_s, L_r, L_m = stator and rotor self-inductances and magnetizing inductance

$L_{s\sigma}$, $L_{r\sigma}$ = stator and rotor leakage inductance

L_{SG}, L_{cable} = equivalent inductance of the synchronous generator and the transmission line

L_{TR}, L_{SH} = short-circuit inductance of the main and the voltage dip transformer

N = number of turns in the coil

n_c = total number of coil sides in the winding

n_N = generator nominal speed

p = number of pole pairs

P_{grid} = grid active power

$\text{PF}_{\text{\_ref}}$ = reference power factor

P_{mec} = mechanical power

P_{N} = rated power of induction generator

R = blade radius

R_{crow} = crowbar resistor

R_{c} = total resistance of the coil

R_{s}, R_{r} = stator and rotor resistances of the phase windings

R_{SG}, R_{cable} = equivalent resistance of the synchronous generator and the transmission line

R_{TR}, R_{SH} = short-circuit resistance of the main and the voltage dip transformers

Q_{grid} = grid reactive power

Q_{ref} = desired reactive power

S_{w} = cross-section area of the coil

T_{e}, T_{gen} = induction generator electromagnetic torque

$T_{\text{e\_ref}}$ = reference electromagnetic torque

T_{L} = external load torque

T_{servo} = time constant of the servo mechanism

T_{shaft} = mechanical torque of the shaft system

U_{crow} = voltage over the crowbar resistor

U_{dc} = dc link voltage

$U_{\text{N,s}}$, U_{N} = generator rated stator voltage

$U_{\text{max,r}}$ = generator maximum rotor voltage

u_{w} = phase voltage

$\underline{v}_s$, $\underline{v}_{\text{r}}$ = space vectors of stator and rotor voltage

v_{∞} = wind speed

β_{k} = either positive or negative multiplier according to the orientation of the coil side

ψ = flux linkage

$\underline{\psi}_s$, $\underline{\psi}_r$ = space vectors of the stator and rotor flux linkages

$\hat{\psi}_{r\_x}$, $\hat{\psi}_{r\_y}$ = estimated rotor flux components in the reference frame fixed to the rotor

$\hat{\psi}_{sx\_r}$, $\hat{\psi}_{sy\_r}$ = estimated stator flux components in the reference frame fixed to the rotor

$\left|\hat{\psi}_{grid}\right|$ = magnitude of the grid flux estimate

$|\psi_{r\_ref}|$ = desired rotor flux command

λ = tip speed ratio

θ = pitch angle

θ_r = generator rotor position

θ_k = angular difference between the two ends of the flexible shaft

ρ = air density

ω_k, ω_m = angular speed of the reference frame, mechanical angular speed of the rotor

ω_r, ω_s = electrical angular speed of the rotor, angular speed of the stator field

Ω = rotational speed of the wind turbine, cross-section of the air gap

σ = conductivity

ν = reluctivity

τ_s = time constant of the first-order discrete filter

Superscripts and subscripts:

dc = direct current

meas = measured

ref = reference

* = complex conjugate

‘ = referred value

ave = average

Abbreviations:

ABS = absolute value

DFIG = doubly fed induction generator

DTC = direct torque control

FEM = finite element method

IM = induction machine

PI = proportional-integral controller

PWM = pulse width modulation

IGBT = insulated gate bipolar transistor

TR = transformer

1 Introduction

1.1 Background to the study

The progress of wind energy around the world in recent years has been consistently impressive. The cumulative global wind power capacity has grown to 46 GW of electricity-generating wind turbines that are operating in over 50 countries. Of these, over 70% have been installed in EU countries. Under international agreements, the penetration is expected to be faster and 10% of the saturation level to have been achieved by the year 2016. The expected saturation level of 1900 GW of wind turbine capacity installed world-wide will be reached in the years 2030-2035 (Herbert et al. 2005).

In the recent period, Finland has also become more interested in using wind energy. The total wind energy capacities installed in Finland up till the end of 1999 were only 38 MW. By the end of the year 2004, the installed wind power capacity was about 82 MW. The target for the year 2010 is about 300 MW, which means that the amount of energy supplied to the Finnish national grid from wind turbines should increase very rapidly (Herbert et al. 2005).

The two basic types of wind turbines used nowadays are

- Fixed-speed wind turbines
- Variable-speed wind turbines.

Fixed-speed wind turbines are mainly equipped with squirrel-cage induction generators, which are also known as self-excited generators (Singh 2003). Self-excited generators work within a limited wind speed range, which is one of their main drawbacks in comparison with variable-speed wind turbines. They can be manufactured as one- or two-speed versions and they are suitable for low power ranges up to 2 MW.

The majority of modern megawatt wind turbines are variable-speed wind turbines equipped with a Doubly Fed Induction Generator (DFIG) that is coupled to the power grid via a main transformer and supplied to the rotor from a frequency converter, as shown in Figure 1.

The main advantage of DFIG wind turbines is their ability to supply power at a constant voltage and frequency while the rotor speed varies. The DFIG concept of a variable-speed wind turbine also makes possible the controlling of the active and reactive power, which is a significant advantage as regards grid integration (Muller et al. 2002).

On the other hand, DFIG wind turbines cause some problems during a grid fault when their rotor circuit, together with the frequency converter, is exposed to a high over-current that is induced by a high transient stator current. In this case, the wind turbine should be disconnected

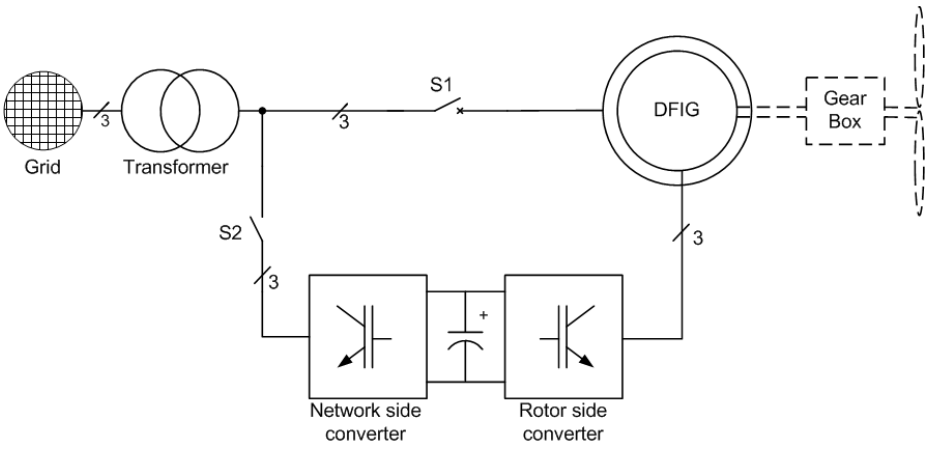

Figure 1. Overall structure of wind turbine with DFIG.

from the network in order to avoid some damage to the electrical or mechanical part of the wind turbine. However, this solution is not acceptable in the case of short-term grid disturbances due to possible grid stability problems and thus some active protection system needs to be applied to keep the turbine connected to the network but also protected against any over-current.

The increase in the number of DFIG wind turbines connected to the network has caused new network codes to be issued, prescribing how a wind generator has to support the network during power disturbances in the network (E.ON Netz 2003, Eltra 2004a). The requirements described in the grid codes mean that a DFIG should behave more or less in the same way as a conventional synchronous generator from the grid integration point of view.

The requirements specified by the new grid codes for the operation of DFIG wind turbines under a grid fault have led to a need to carry out accurate transient simulations in order to understand the impact of power system disturbances on wind turbine operation. The simulation studies that have been performed and presented in the recent literature are focused mainly on the transient behavior of a DFIG during a balanced grid disturbance and on fault ride-through capability studies. The literature review of Salman et al. (2004) concludes that it is necessary to model a DFIG and the associated control and protection circuits adequately, especially in the event of a fault.

The simulation studies have mostly been carried out by using commercial transient simulation software such as a Matlab-Simulink system simulator (Iov et al. 2004) and power system simulators such as PSS/E (Lei et al. 2006) or PSCAD (Hogdahl and Nielsen 2005), as well as DIgSILENT (Hansen et al. 2004, Pöller 2003). These commercially available simulation programs offer numerous possibilities to choose the most adequate model representing DFIG, drive train and the control system of the DFIG from the built-in blocksets. However, the standard models of the DFIG included in the simulation software are, in many cases, inadequate from the accuracy point of view as a result of simplifications such as

neglecting the dc stator transients' components, leakage inductance saturation, mutual inductance saturation, and electromagnetic transients. This makes them unsuitable for representing the transient performance of a DFIG accurately in the event of a grid fault. The simulation of a power system with a DFIG under unbalanced faults by means of conventional analytical models may also be problematic. These studies require a different representation of DFIG than in the case of a balanced fault. The method of symmetrical components presented by Krause et al. (1995) is suggested for use in the analysis of unbalanced DFIG operation when taking into account the zero-sequence components.

1.2 Aim of the work

The main objective of this work was to develop and experimentally validate a coupled field-circuit transient simulator of a wind energy conversion system with a DFIG. This study is focused mainly on:

- The transient and ride-through analysis of a wind-power DFIG under balanced and unbalanced network disturbances, using the developed field-circuit simulator.

- An investigation of the consequences of the different modeling approaches on the transient analysis accuracy of a DFIG wind turbine under a grid disturbance.

- An investigation of the influence of crowbar operation on the transient behavior of a wind-power DFIG.

- An investigation of the impact of detailed DFIG wind turbine modeling on the accuracy of electrical system performance analysis in the case of a short-term grid disturbance analysis.

1.3 The scientific contribution of this work

- Applying the developed methodology of combining FEM computation with a Matlab-Simulink simulator for the dynamic modeling of the whole electric drive system and electric part of a wind energy conversion system.

- Verification of the method for coupling the magnetic field equations of the electrical machine with circuit equations of the windings and external electric circuits.

- Transient behavior and ride-through analysis of a DFIG during balanced and unbalanced grid disturbances using the coupled field-circuit simulator.

- Investigation of the impact of passive and active crowbar operation on wind-power generator behavior during a grid fault.

- Comparative study of different variable speed wind turbine modeling approaches from the point of view of transient simulation accuracy.

- Experimental validation of the developed field-circuit simulator by means of a full-scale test on a 1.7-MW doubly fed wind-power induction generator connected to the laboratory grid and supplied to the rotor from the DTC-controlled and crowbar-protected frequency converter during a grid disturbance.

Each of the items in the list above is discussed in this summary of publications.

This work was carried out within the framework of a long-term project focused on the development and verification of a method for coupling the magnetic field equations of an electrical machine with the circuit equations of the windings and external electric circuits. The main part of the project work was divided between Sami Kanerva and Slavomir Seman. Kanerva developed the coupled field circuit simulator in Matlab-Simulink and he made the comparison of the different methods of coupling. Seman contributed to this part of the work by testing the methods and creating the simulation models in the Matlab-Simulink environment, as stated in the preface of the dissertation (Kanerva 2005). In Chapter 5.2 of the doctoral thesis (Kanerva 2005), a case study of a wind-power DFIG under a network disturbance is presented. The results presented in this section were obtained from the system model developed by Seman, which was coupled with the different DFIG FEM models developed by Kanerva in order to compare different methods for the field circuit coupling (Publication P3).

1.4 Publications

The publications are listed in order of completion:

Publication P1

The paper presents the transient performance study of a 1.7-MW wind-power doubly fed induction generator (DFIG) during a network fault using a MATLAB-Simulink-based simulator. The simulator consists of the DFIG analytical model, a detailed model of a DTC-controlled frequency converter including passive crowbar protection, and a model of the main transformer. The results show the transient behavior of the doubly fed induction generator when a sudden voltage dip is introduced, with and without the crowbar implemented.

The main contribution of this paper is the presentation of the wind generator simulator developed in Matlab-Simulink and used for the transient analysis of a DFIG during a grid disturbance. In the paper, the impact of passive crowbar operation on wind-power generator behavior during a grid fault is also studied.

Seman wrote the paper. The co-authors, Niiranen, Kanerva, and Arkkio, contributed to the

paper with several discussions and valuable comments. Seman developed the wind-power generation system simulator in Matlab-Simulink on the basis of information published in Gokhale et al. (2004) and part of the simulation code provided by Niiranen.

Publication P2

The paper presents the transient analysis of a wind-power doubly fed induction generator during power system disturbances. A finite element model of an induction machine coupled with a circuit model of a frequency converter is applied in order to model the DFIG, and, together with a model of the transformer, network, and control, represents the wind-power generator with a DFIG described in Publication P1. The transient currents and electromagnetic torque obtained from the DFIG finite element model are compared with the simulation results obtained by means of an equivalent circuit-based analytical model with constant lumped parameters.

The main contribution of this paper is the description of the coupled field-circuit simulator that is used in the transient behavior study of a DFIG under a grid disturbance. The field-circuit simulator is benchmarked with a wind-power DFIG simulator based on a simplified analytical model.

Seman wrote the paper. Kanerva wrote Chapter 2, in which he describes the coupling of the FEM solver and system simulator. The co-authors, Niiranen and Arkkio, contributed to the paper with several valuable comments.

Publication P3

This paper presents a method for coupling the magnetic field equations of the electrical machine with the circuit equations of the windings and external electric circuits. The electrical machine is modeled by means of electromotive force and dynamic inductance, which are determined by the finite element method (FEM) and updated at each time step of the transient simulation. The external circuit model is solved with system simulation software, using the parameters obtained by the FEM. The method is verified by simulating a doubly fed induction generator in steady state and a three-phase short circuit and comparing the results with those obtained by the directly coupled field circuit method presented in Publication P2.

The main contribution of the paper is to show that the method developed for coupling the magnetic field equations of the electrical machine with the circuit equations of the windings and external electric circuits is also applicable to complex systems. This is verified by a transient simulation of a wind-power doubly fed induction generator under a grid disturbance.

Kanerva wrote the paper. Seman contributed to the paper by providing the simulation model of a complex wind-power generation system that was used for the validation of the field circuit coupling method proposed by Kanerva. Arkkio contributed to the paper with several discussions and valuable comments.

Publication P4

This paper presents the transient performance study of a 1.7-MW wind-power doubly fed induction generator when a sudden voltage dip is introduced using the field-circuit simulator. The field-circuit simulator used for transient simulation in Publication 2 is experimentally validated by means of a full-power test.

The main contribution of this paper is the experimental verification of the developed field-circuit transient simulator used for the transient simulation of a doubly fed wind-power induction generator connected to the grid and controlled by a modified direct torque control during a power system disturbance.

Seman wrote the paper in close co-operation with Niiranen, who provided all the necessary technical and measured data. The measurements were carried out at the test field of ABB Oy, Finland. Kanerva contributed to the paper with a description of the finite element model of the DFIG. The co-authors, Arkkio and Saitz, contributed to the paper with several discussions and valuable comments.

Publication P5

This paper presents a variable-speed 2 MW DFIG wind turbine simulator. The detailed model of the wind turbine includes, in addition to the previously presented models in Publications 2 and 4, a wind turbine aerodynamic model, wind turbine control and drive train model. The simulation results obtained by means of the detailed wind turbine model are compared with the results obtained from a simplified simulator with an analytical model and FEM model of the DFIG. A comparison of the simulation results shows the influence of the detailed wind turbine and advanced DFIG modeling on the accuracy of the transient simulation during a short-term grid disturbance.

The main contribution of the paper is to provide a comparative study of different variable-speed wind turbine modeling approaches from the transient simulation accuracy point of view.

Seman wrote the paper in co-operation with Iov. Iov provided the technical data and information about the aerodynamic and mechanical models and variable-speed wind turbine control algorithms. The co-authors, Niiranen and Arkkio, contributed to the paper with valuable comments.

Publication P6

This paper presents a ride through the operation analysis of a wind-power DFIG using a coupled field-circuit simulator. The impact of a two-phase asymmetrical grid fault on DFIG generator operation and the ride-through capability of the DFIG wind-power generation system is studied by simulation. This study extends the balanced fault studies presented in Publications P1-

P5. The developed active crowbar model is also described, which, in comparison with the passive crowbar presented in Publication 1, allows the ride-through of a wind-power DFIG with the possibility of supplying reactive power into the grid during long-term voltage dips.

The main contribution of this paper is the validation of the suitability of the field circuit simulator for use for the ride-through operation analysis of a DFIG wind-power generator in the case of an asymmetrical network disturbance. The paper reveals the influence of the saturation phenomena on the transient behavior of an active crowbar-protected and direct torque-controlled wind-power generator.

Seman wrote the paper in co-operation with Niiranen, who provided all the necessary technical data. The co-author, Arkkio, contributed to the paper with several discussions and valuable comments.

1.5 Structure of the work

A detailed literature review, presented in Chapter 2, is focused mainly on the state of the art of the DFIG modeling methods used in wind turbine transient studies. An overview of the frequency converter models and control algorithms used for the analysis of DFIG wind turbines is presented in Chapter 3, together with a short description of the network model used in the study. Chapter 4 presents a short review of the literature on variable-speed wind turbine modeling, with a description of an aerodynamics model, shaft system model, and model of a wind turbine control system. A short literature overview of grid codes is presented in Chapter 5. The same chapter also presents the state of the art regarding the transient and ride-through analysis of DFIG, as well as a short description of the studied cases. Chapter 6 describes the experimental set-up used to obtain the experimental results that are presented in Publication P4. Chapter 7 is dedicated to discussion of the results and concludes the thesis.

2 Modeling of the doubly fed induction machine

A DFIG is a main part of the wind turbine, in which the mechanical energy transmitted by a shaft system is converted to electrical energy and thus, in the case of transient studies, the DFIG should be modeled accurately. A common modeling approach is to represent a DFIG by means of an equivalent circuit-based analytical model with lumped parameters. Another option is to use a Finite Element Method (FEM) model. Both approaches will be described briefly in the following sections. The coupled field-circuit simulation approach, as a rather new method of analysis, especially in the field of wind-power generation transient analysis, will also be briefly discussed.

2.1 Analytical model

Most of the dynamic analytical models of an induction machine (IM) are derived on the basis of two basic topologies of the equivalent circuit. The conventional "T" equivalent circuit shown in Figure 2 is commonly used in the literature (Vas 1992), while the simplified "Γ" is used for the derivation of the control strategies (Hinkkanen 2004).

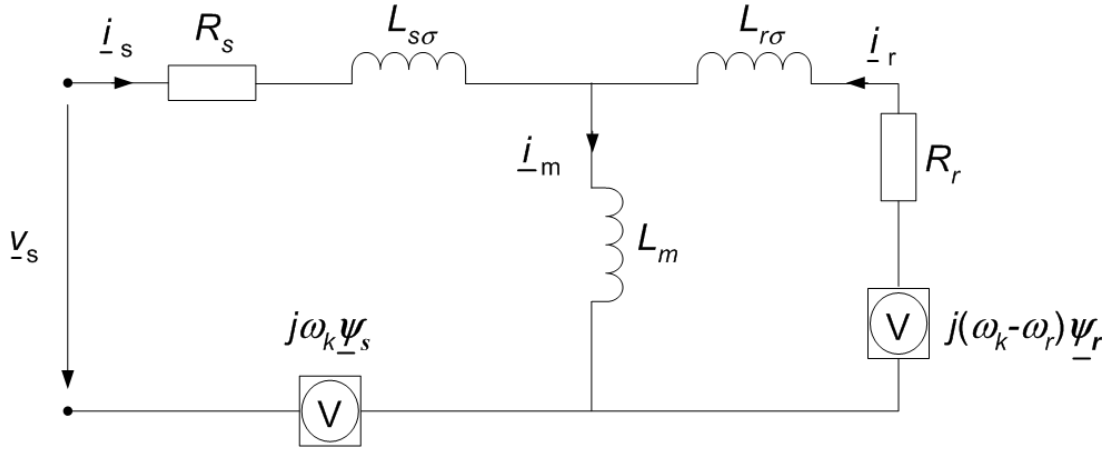

Figure 2. Dynamic "T" equivalent circuit of induction machine.

On the basis of the equivalent circuit presented, we can derive the voltage equations of the IM in a general reference frame using the space vector approach (Kovácz and Rácz 1959)

$$\underline{v}_s = R_s \underline{i}_s + \frac{d\underline{\psi}_s}{dt} + j\omega_k \underline{\psi}_s \tag{2.1}$$

$$\underline{v}_r = R_r \underline{i}_r + \frac{d\underline{\psi}_r}{dt} + j(\omega_k - \omega_r)\underline{\psi}_r \tag{2.2}$$

where symbol $\underline{v}_s$ represents the stator voltage space vector in the general reference frame, $\underline{i}_s$ the space vector of the stator current in the general reference frame. Similarly, $\underline{v}_r$ and $\underline{i}_r$ are the space vectors of the rotor voltage and current. The stator and rotor resistances of the phase

windings are denoted by the symbols R_s and R_r, respectively. The angular speed of the reference frame is ω_k and the electrical angular speed of the rotor is ω_r. The space vectors of the stator and rotor flux linkages under linear magnetic conditions are defined as

$$\underline{\psi}_s = L_s \underline{i}_s + L_m \underline{i}_r \tag{2.3}$$

$$\underline{\psi}_r = L_r \underline{i}_r + L_m \underline{i}_s \tag{2.4}$$

where L_s and L_r are the stator and rotor self-inductances, respectively, and L_m is the magnetizing inductance. If we define the space vector of the magnetizing current as the sum of the space vectors of the stator $\underline{i}_s$ and the rotor $\underline{i}_r$ current,

$$\underline{i}_m = \underline{i}_s + \underline{i}_r \tag{2.5}$$

we can express the flux linkages

$$\underline{\psi}_s = L_m \underline{i}_m + L_{s\sigma} \underline{i}_s \tag{2.6}$$

$$\underline{\psi}_r = L_m \underline{i}_m + L_{r\sigma} \underline{i}_r \tag{2.7}$$

where $L_{s\sigma}$ and $L_{r\sigma}$ denote the stator and rotor leakage inductances, respectively.

The electromagnetic torque is given by

$$T_e = \frac{3}{2} p \operatorname{Im}\left\{ \underline{i}_s \underline{\psi}_s^* \right\} \tag{2.8}$$

where p is the number of pole pairs and the complex conjugate is denoted by the symbol *.

The equation of the motion is

$$\frac{d\omega_m}{dt} = \frac{1}{J}\left(T_e - T_L\right). \tag{2.9}$$

where symbol ω_m expresses the mechanical angular speed of the rotor, J is the rotor moment of inertia, and T_L is an external load torque.

The stator and rotor voltage equations, together with the equation of motion, will determine the transient performance of the induction machine. For this purpose, a two-axis system of the different co-ordination systems is used to obtain a system of the differential equations that can be solved by the application of numerical methods.

The IM can be modeled in any frame of reference; however, there are three reference frames that are commonly used (Krause et al. 1995). The voltage equations of the induction machine in the stationary, rotor, or synchronously rotating reference frames can be obtained by assigning the appropriate value to ω_k in the voltage equations (2.1) and (2.2). The stationary reference frame is defined by assigning ω_k=0, in the case of the rotor reference frames ω_k=ω_r and ω_k=ω_s when the synchronously rotated reference frame is employed.

The dynamic model of an induction machine above is usually presented by means of a so-called fifth-order model (Stanley 1938) that represents IM by a system of five general differential equations of an idealized induction machine. In some power system studies, it is desirable to reduce the complexity of the system by using reduced-order models that can be obtained by assuming some of the derivatives as being equal to zero (Thiringer and Luomi 2001). For example, a third-order model of IM is obtained when we neglect the stator flux transients, as shown by Ledesma and Usaola (2004).

The doubly fed induction generator used in variable-speed wind turbines is frequently represented by a conventional dynamic fifth-order model of IM in a two-axis d-q reference frame rotating at synchronous speed (Akhmatov 2002) or in a rotor reference frame (Chellapilla and Chowdhury 2003). According to the discussion in Tapia et al. (2003), in order to express DFIG dynamic behavior as realistically as possible, the "Quadrature-Phase Slip Ring" frame, where the stator and rotor variables are referred to their own corresponding reference frames, should be employed. A rather common DFIG model is the so-called "voltage behind reactance" reduced dynamic model (Holdsworth et al. 2003a, Nunes et al. 2004), which is widely used in the analysis of power system faults. In the case of transient stability studies, it is rather common to reduce the fifth-order model to a third-order model (Ekanayake et al. 2003a, Ledesma and Usaola 2005). However, as concluded in Akhmatov (2002), using third-order models may result in too-low transient currents during disturbances, which may lead to inaccurate results, especially when the transient behavior of a DFIG wind turbine during a grid fault is being studied.

The dynamic DFIG model used in this study is of fifth-order, with constant lumped parameters. The machine equations are written in a x-y reference frame fixed to the rotor. A detailed description of the DFIG dynamic model is presented in Publication P1 and Publication P4.

2.2 Finite element model

The analytical model of the induction machine is a rather simplified representation of a complex electromagnetic system that usually does not represent detailed phenomena such as, for example, the magnetic saturation or rotor current displacement resulting from the skin effect. Using an FEM-based model of IM can eliminate this drawback of the analytical model. However, using the FEM in the simulation of the transient behavior of an IM is computationally a time-demanding task, but, on the other hand, present-day computers allow the FEM to be utilized even for the transient analysis of such a complex system as a DFIG wind turbine.

The magnetic field in the DFIG can be modeled by two-dimensional finite element analysis and coupled with the voltage equations of the windings (Arkkio 1987). The z-component of the magnetic vector potential A satisfies

$$\nabla \cdot (\nu \nabla A) - \sigma \frac{\mathrm{d}}{\mathrm{d}t} A + \frac{N i_{\mathrm{w}}}{S_{\mathrm{w}}} = 0 \tag{2.10}$$

where ν is the nonlinear reluctivity, σ is the conductivity, and N is the number of turns in a coil with a cross-section area S_{w} and carrying a phase current i_{w}. Since there are no damping bars in the DFIG rotor and the conductivity in the laminated iron core is set to zero, the derivative term in (2.10) only covers the effect of eddy currents in the steel shaft. The voltage equations for the windings take the form

$$u_{\mathrm{w}} = \sum_{k=1}^{n_{\mathrm{c}}} \beta_k l_k \frac{\mathrm{d}}{\mathrm{d}t} A_k^{\mathrm{ave}} + R_c i_{\mathrm{w}} + L_{\mathrm{e}} \frac{\mathrm{d}}{\mathrm{d}t} i_{\mathrm{w}} \tag{2.11}$$

where u_{w} is the phase voltage, n_{c} is the total number of coil sides in the winding, β_k is either a positive or negative multiplier according to the orientation of the coil side, l_{k} is the length of the coil side, A_k^{ave} is the average vector potential on the coil side, R_c is the total resistance of the coil, and L_{e} is the additional end-winding inductance.

The flux linkage ψ is determined by adding together the contributions of all coil sides in the winding

$$\psi = \sum_{k=1}^{n_{\mathrm{c}}} \beta_k A_k^{\mathrm{ave}} l_k \tag{2.12}$$

The sources of the field analysis are the voltages applied in the phase windings in the stator and rotor. The magnetic vector potential and phase currents are obtained from the simultaneous solution of the above equations.

The electromagnetic torque T_{e} is determined from the field solution using the virtual work principle

$$T_{\mathrm{e}} = l_e \frac{\mathrm{d}}{\mathrm{d}\theta_r} \int_{\Omega} \int_0^H \boldsymbol{B} \cdot \mathrm{d}\boldsymbol{H} \ \mathrm{d}\Omega \tag{2.13}$$

where l_e is the axial length, θ_r is the position angle of the rotor and Ω is the cross-section of the air gap. The magnetic flux density $\boldsymbol{B}$ and the magnetic field strength $\boldsymbol{H}$ are determined from the field solution. The angular speed of the rotor can be considered as constant or solved by the equations of motion.

The mechanical angular speed ω_{m} and position of the rotor θ_r are solved from

$$\omega_{\mathrm{m}} = \int \frac{1}{J} (T_{\mathrm{e}} - T_{\mathrm{L}}) \mathrm{d}t \tag{2.14}$$

$$\theta_r = \int \omega_{\mathrm{m}} \mathrm{d}t \tag{2.15}$$

where J is the moment of inertia and T_{L} is the load torque. The movement of the rotor is modeled by modifying the air-gap finite element mesh.

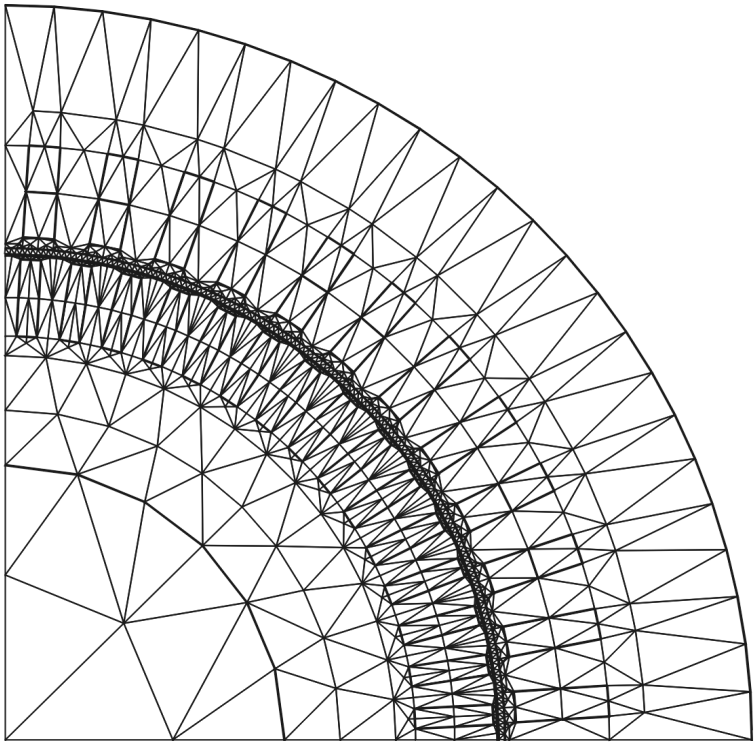

Figure 3. Finite element mesh of the 1.7-MW doubly fed induction generator.

The induction machine is specified by a two-dimensional geometry that is covered by a finite element mesh, which consists of 1245 nodes forming 1848 first-order triangular elements. If possible, the cross-section of the machine geometry can be divided into symmetry sectors, as shown in Figure 3, and only one is calculated by the FEM and the symmetry constraints are set on the periodic boundary. The stator and rotor windings are modeled as series-connected coils with a uniform current density. A detailed description of the FEM model and numerical methods used for the calculation of the magnetic field is presented by Kanerva (2005).

2.3 Field-circuit simulator

The methods used for coupling the field (FEM) solver with the system or circuit simulator can, in general, be divided into two main groups, direct and indirect. In the case of the direct coupling method, the field and circuit equations are solved simultaneously, while in the case of indirect coupling, the field and circuit equations are solved sequentially. A detailed literature overview of direct and indirect coupling methods can be found in Kanerva (2005). No transient study of a wind-power generation system using the coupled field-circuit approach has yet been presented in the literature except the study of Runcos et al. (2004). In this study, a prototype of a 100-kW Brushless Doubly Fed Induction Generator for wind-power conversion application is investigated by means of a direct coupling method developed by Oliviera et al. (2002).

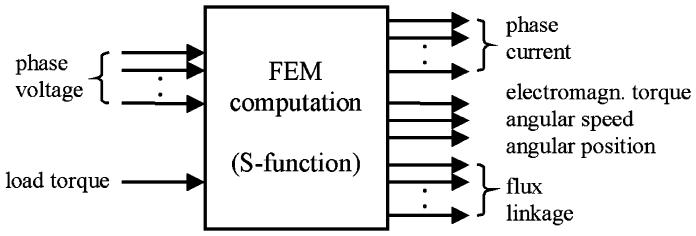

Figure 4. Functional block of the FEM computation.

The coupling between the FEM and circuit simulator is, in the present work, realized by an indirect coupling method, except in the comparative study presented in Publication P3, where the circuit parameter approach is introduced and compared with the current output approach. As concluded in Publication P3, the circuit parameter approach exhibits some drawbacks, such as a slightly higher time consumption and possible numerical instability without additional filtering. The method is the most beneficial in those cases where the external circuit is relatively complex and consists mostly of passive circuit elements. For plain impedance in series with the windings, the current output approach is a simpler approach and thus this was used in the further analyses of the DFIG wind-power generator.

The coupled field-circuit model used in this work is described in detail and verified by the transient simulation of the DTC motor drive in Kanerva et al. (2003). The FEM model of the induction machine represents the model as a Matlab-Simulink functional block shown in Figure 4, using a dynamically linked program code S-function. The voltages of the phase windings in the stator and rotor are given as input variables and the phase currents, electromagnetic torque, rotor position, and flux linkage in the stator and rotor are obtained as output variables.

The initialization of the magnetic field is performed before the simulation; the initial magnetic field in the electrical machine must be established. This can be done by time-harmonic steady-state analysis when sinusoidal voltages and currents are assumed (Arkkio 1987). The information about the magnetic field and finite element mesh is stored in a text file or Matlab's MAT file, which is read by the S-function at the beginning of the simulation. After the time-stepping simulation, the magnetic field is stored in a new file that can be used as the initial condition for a new simulation.

The simulation parameters of Simulink and the special parameters of the S-function are given by the user before the simulation. The user has to specify whether the stator is connected in star or delta, whether the end-ring impedance of the rotor cage is taken into account, the time step length for the FEM computation, and the file names for the storage of the initial and final magnetic fields. An intermediate file transfers these settings from Simulink to the FEM block.

The overall system structure employs either variable or fixed steps, which are governed by Simulink. Respectively, the S-function for the FEM computation uses fixed time steps, which override Simulink's own steps and are set by the user. Because the steps for the FEM model are usually longer than the steps in the overall system model, they are considered as major steps and Simulink's own steps are considered as minor steps.

The procedure of the FEM solution in the S-function is presented in Figure 5. The output of the FEM block is calculated in major steps only and it remains constant during the minor steps. As a result, the variables in the overall system model may vary freely during the minor steps, with no immediate feedback from the FEM model. This is called weak coupling and it is suitable for systems in which the phenomena of different time scales are coupled.

The step size for the FEM computation must be selected carefully in order to gain both effective computation and accurate results. In spite of the indirect coupling, the accuracy of the coupled solution can be maintained by choosing the time steps appropriately according to the physical time constants. By using short steps in the converter model and longer steps in the FEM model, the time-stepping simulation is also more efficient, because the time-consuming FEM solution is not determined too frequently.

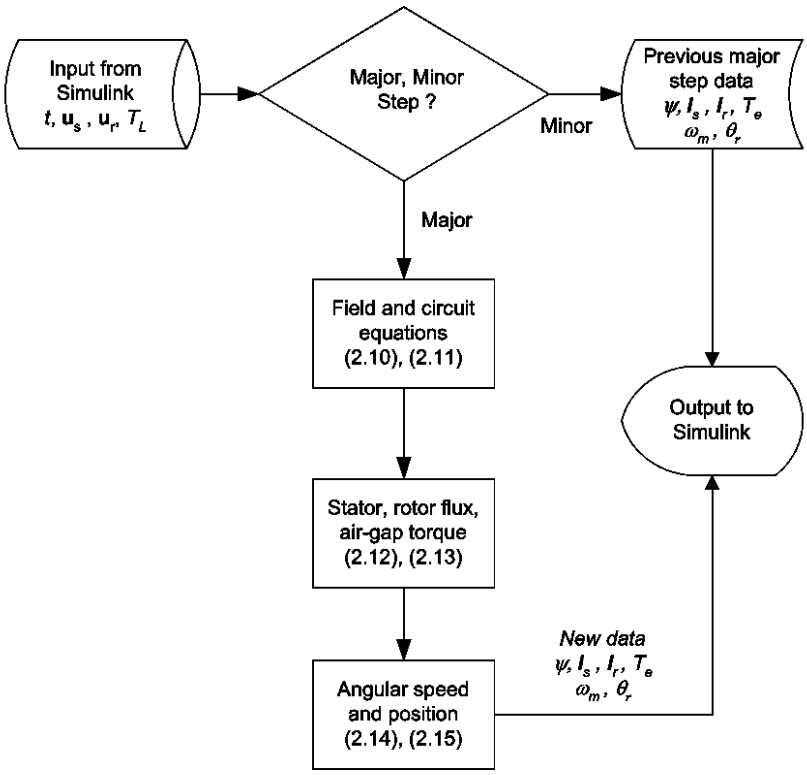

Figure 5. The coupled simulator computational algorithm.

3 Modeling of the frequency converter and power system

The doubly fed induction machine can be operated either as a generator or motor at both a sub-synchronous and super-synchronous speed. In the case of wind-power induction generators, the induction machine operates only in a generating mode at sub-synchronous and super-synchronous speeds where the speed range is limited by the maximum voltage of the rotor-side frequency converter. The DFIG is supplied to the rotor from a frequency converter consisting of back-to-back connected converter bridges with a dc intermediate link, as depicted in Figure 6.

The network-side converter operates at a network frequency and controls the voltage level in the dc link circuit. It can also deliver reactive power to the supply system if required. The rotor-side frequency converter operates at different frequencies, depending on the rotor speed, and controls the flux of the DFIG and thus the active and reactive power. The frequency converters that are capable of the ride-through usually also include an over-current protection, a so-called crowbar, which protects the rotor-side converter, as well as the rotor circuit of the DFIG, against high currents during grid disturbances.

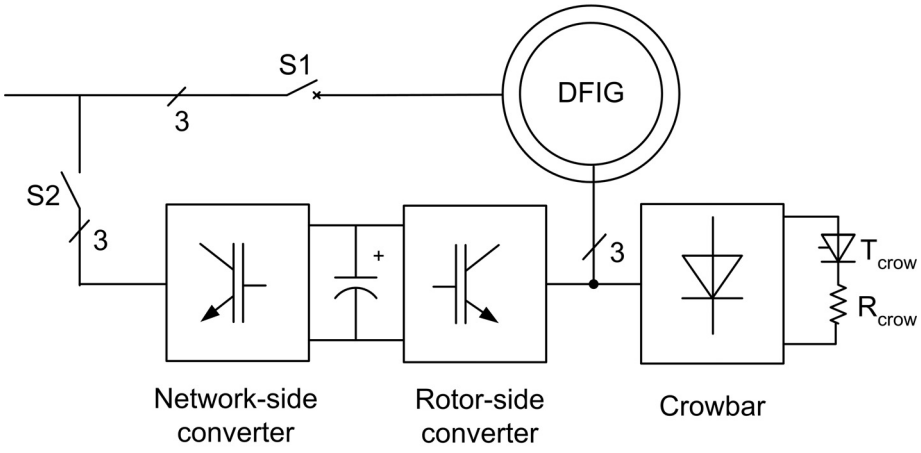

Figure 6. The frequency converter equipped with crowbar.

3.1 Network-side frequency converter

The network-side frequency converter is usually represented by a simplified model, a so-called generic control scheme based on a set of PI controllers used for obtaining two-axis voltage values depending on the required network active and reactive power values (Pöller 2003). These models neglect the switching dynamics of the converter and an ideal control is assumed, meaning that the converter is able to follow its demanded value at any time (Akhmatov 2002).

A detailed model of the network-side frequency converter is presented by Pena et al. (1996), where the vector control approach is used, with a reference frame oriented along the supply voltage vector position, making possible independent active and reactive power flow between the network and the network-side converter. The converter is current regulated using a standard asymmetric sampling PWM scheme. A similar approach is used in Abbey and Joós (2004) and in Abolhassani et al. (2003), where a field-oriented control aligned with the stator voltage vector position is employed. The network-side converter could also be controlled as shown by Pöllänen (2003), where a modified DTC is used to control the active and reactive power of the network-side converter. A detailed model of the network-side vector-controlled frequency converter that uses hysteresis modulation is presented in Chowdhury and Chellapilla (2006) and a space-vector PWM modulation is applied in Gómez and Amenedo (2002).

Akhmatov (2003) states as a conclusion that when we study a DFIG wind turbine under network disturbances, it is necessary also to model the network-side frequency converter in detail. The author stresses that if we neglect the network-side converter model, it would affect the accuracy of the rotor current calculation as well as the dc link voltage, which are monitored by a protective system, and that this could significantly affect the accuracy of the simulation.

However, the majority of DFIG wind turbine studies omit the model of the grid-side converter and the dc link voltage is considered as constant (Arnalte et al. 2002, Tapia et al. 2003, Nunes et al. 2004). A compromise solution between the detailed model of the network-side converter and constant dc link voltage consideration could be the approach presented in Ledesma and Usaola (2005), where a simplified dc link voltage controller is implemented. This method is based on the calculation of the dc link capacitor voltage as a function of the input power to the dc link.

The network-side converter is modeled in this study by a simplified model, which is shown in Figure 7. The network-side converter is represented in simulation by a discrete transfer function where τ_s denotes the time constant of the first-order discrete filter. The symbols I_{rot} and I_{net} denote the dc currents flowing between the dc link and the rotor-side converter and the dc link and network-side converter, respectively. The aim of the control of the network-side inverter is to maintain the level of dc link voltage U_{dc} at a pre-set value $U_{\mathrm{dc\_ref.}}$. A PI controller with a limiter controls U_{dc}. The limits of the PI controller are adapted to the monitored amplitude of the grid voltage.

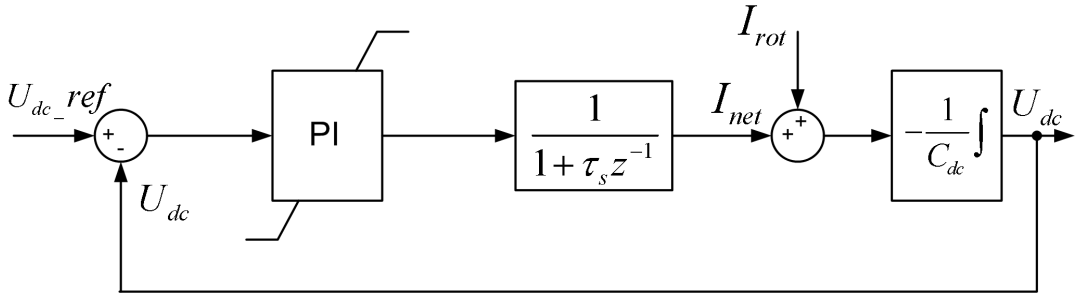

Figure 7. Simplified model of the network-side converter.

3.2 Rotor-side frequency converter

Similarly to the case of the network-side converter, the rotor-side converter can also be represented by several modeling approaches. The most common model of the rotor-side converter is based on the stator flux-oriented vector control scheme, where the active and reactive power are controlled as presented in Yamamoto and Motoyoshi (1991). The switching dynamics could be represented by including a PWM modulator into the model, as shown by Pena et al. (1996) and Tapia et al. (2003) or by using a hysteresis modulator (Chowdhurry and Chelapila 2006) to control the switching of the IGBT inverter bridge. A space vector-modulated matrix converter with a stator-flux vector control has been proposed for DFIG rotor current control by Zhang et al. (1997).

A generic control scheme could also be applied to the rotor-side converter (Akhmatov 2002), with two series of two frequency converters when the switching dynamics are neglected, assuming that the rotor-side converter perfectly follows the reference values (Pöller 2003). The rotor-side converter in Lei et al. (2006) is simplified in such a way that the converter is modeled as an ideal voltage source.

An alternative control scheme to the vector control is direct torque control (DTC) (Takahasi and Nugushi 1986). The application of DTC to DFIG control was presented in Arnalte et al. (2002). A modified DTC strategy-based controller for a DFIG wind turbine is described in detail by Gokhale et al. (2004).

The rotor-side frequency converter used in this work utilizes modified DTC, which is represented by a detailed model including the switching dynamics, hysteresis control, and detailed control algorithms; its control structure is depicted in Figure 8. The modified DTC control is a simpler control method than the vector control and exhibits lower machine parameter dependence. The DTC can control the flux and torque directly, while the voltage and currents are controlled indirectly, unlike in vector control. The rotor-side converter is controlled by means of two hysteresis controllers that define the switching pattern on the basis of an optimal switching table.

The magnitude of the rotor flux estimate $|\hat{\psi}_r|$ is obtained by absolute value block calculation based on the rotor fluxes calculated by the Torque and Flux calculator as

$$|\hat{\psi}_r| = \sqrt{(\hat{\psi}_{r\_x})^2 + (\hat{\psi}_{r\_y})^2} \tag{3.1}$$

where the symbols $\hat{\psi}_{r\_x}$ and $\hat{\psi}_{r\_y}$ denote the estimated rotor fluxes in the two axis reference frame fixed to the rotor. The rotor flux estimates are

$$\hat{\psi}_{r\_x} = \frac{L_m}{L_s}\hat{\psi}_{s\,x\_r} + \frac{L_s L_r - L_m^2}{L_s} i_{rx} \tag{3.2}$$

$$\hat{\psi}_{r\_y} = \frac{L_m}{L_s}\hat{\psi}_{s\,y\_r} + \frac{L_s L_r - L_m^2}{L_s} i_{ry} \tag{3.3}$$

where i_{rx} and i_{ry} denote the rotor current components in the two-axis rotational reference frame and $\hat{\psi}_{sx\_r}$ $\hat{\psi}_{sy\_r}$ denote the *x* and *y* components of the stator flux vector estimates in the rotational frame. L_m, L_s, and L_r are the magnetizing, stator, and rotor inductances of DFIG, respectively.

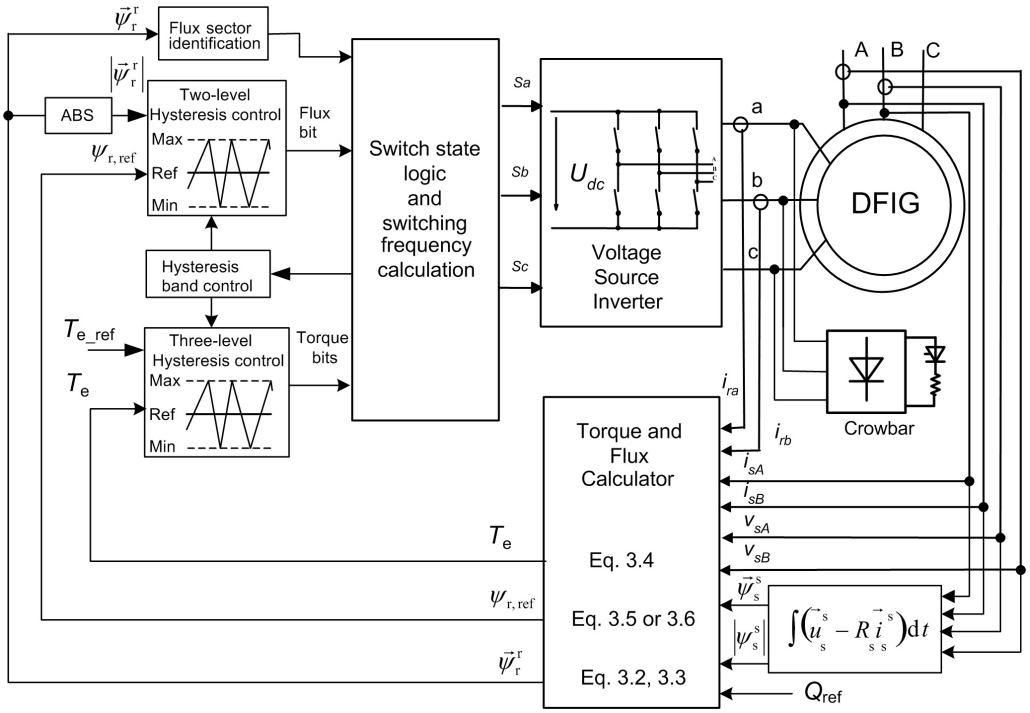

Figure 8. The control structure of the modified DTC.

The stator flux estimates are obtained by the integration of the measured stator voltage after the subtraction of the resistive voltage drop over the stator winding. A rotator transforms the estimated stator flux from the two-axis stator co-ordinates to the two-axis rotor co-ordinate system. The magnitude of the grid flux estimate $|\hat{\psi}_{grid}|$ that is used to control the synchronization of the DFIG with the network is calculated by integrating the measured line-to-line stator voltages transformed into the two-axis reference frame. The estimate of the electromagnetic torque that is an input of the three-level hysteresis comparator is given by

$$\hat{T}_e = \frac{3}{2}\, p\, \frac{L_s L_r - L_m^2}{L_m}\left(\hat{\psi}_{r\_x}\hat{\psi}_{sy\_r} - \hat{\psi}_{r\_y}\hat{\psi}_{sx\_r}\right) \tag{3.4}$$

The reference values of the electromagnetic torque T_{e_ref}, as well as the angular rotor speed ω_r, are considered to be constant. The modulus of the desired rotor flux command $|\psi_{r\_ref}|$ obtained from the reference flux calculator as a function of the desired reactive power Q_{ref}, given torque command T_{e_ref}, electrical frequency of the DFIG stator side ω_e, and grid flux estimate $|\hat{\psi}_{grid}|$ is given as

$$\left|\psi_{r\_ref}\right| = \sqrt{\left(\frac{\left(L_s L_r - L_m^2\right) T_{e\_ref}}{L_m \left|\hat{\psi}_{grid}\right|}\right)^2 + \left(\frac{L_r}{L_m}\left|\hat{\psi}_{grid}\right| + \frac{\left(L_s L_r - L_m^2\right) Q_{ref}}{\omega_e L_m \left|\hat{\psi}_{grid}\right|}\right)^2} \tag{3.5}$$

If the power factor PF_ref is used as a reference value for a control algorithm, the modulus of the desired rotor flux command $\left|\psi_{r\_ref}\right|$ is given as

$$\left|\psi_{r\_ref}\right| = \sqrt{\left(-\frac{(L_s L_r - L_m^2)}{L_s}\frac{T_{e\_ref}}{\left|\psi_{grid}\right|}\right)^2 + \left(-\frac{L_m}{L_r}\left|\psi_{grid}\right| - \frac{T_{e\_ref}}{\left|\psi_{grid}\right|}\frac{\sqrt{1-(PF\_ref)^2}}{PF\_ref}\right)^2} \tag{3.6}$$

The torque and flux hysteresis comparators provide a logical output that is used together with the flux sector identification for switching pattern establishment, defined by the switching state logic. When the switching pattern is established, a voltage vector is applied to the rotor and this voltage will change the rotor flux. The optimal switching frequency f_{sw} is maintained by means of hysteresis band control. The torque and flux hysteresis comparators provide logical output that is used together with $\hat{\psi}_{r\_x}$ and $\hat{\psi}_{r\_y}$ for switching the pattern establishment defined by the switching table, as described in e.g. Arnalte and Burgos (2002). The tangential component of the voltage vector controls the torque, whereas the radial component increases or decreases the flux magnitude. The switching signals control the inverter bridge, which consists of 6 IGBT transistors that are represented in the simulator as ideal switches.

3.3 Rotor over-current protection – Crowbar

The new grid code requirements (E.ON Netz 2003) require a DFIG to remain connected to the network even in the event of a short-term power network disturbance. This, however, causes trouble because high currents are induced to the rotor from the stator side when a stator voltage dip occurs and thus the rotor and rotor-side converter need to be protected against an over-current.

A detailed description of the protective system for the DFIG wind turbine concept can be found in Akhmatov (2003), where the author presents two arrangements for the elimination of an over-current in the rotor circuit. The first method is based on a fast demagnetization of the rotor circuit by switching all the IGBT transistors off. The rotor is short-circuited via inverter diodes and the magnetic energy of the rotor is transferred to the dc link capacitor. The second technique is based on the assumption that, after the rotor-side converter modulation has stopped, the rotor circuit is short-circuited via a finite external resistance.

Xiang et al. (2004) present a theoretical study of a ride-through control method in which a PWM converter eliminates an over-current in the rotor circuit. A similar approach has been analyzed and experimentally verified in Hogdahl and Nielsen (2005). This approach, however, leads to a situation in which the inverter bridge power switches need to be over-sized in order to be able to handle the over-current, which would cause additional losses in the converter.

One possible solution is using a rotor over-current protection, a so-called crowbar, which is connected between the rotor of the DFIG and rotor-side converter. Most of the crowbars in the literature are described as protection which deactivates the rotor-side converter and short-circuits the rotor winding, as presented in Holdsworth et al. (2003a), when the rotor current exceeds the limit value. A similar explanation of the operation of the crowbar is presented by e.g. Ekanayake et al. (2003b), but the operation is not very clearly described. The study presented by Petersson et al. (2005) introduces an over-voltage protection device that, in the event of high rotor currents, short-circuits the rotor. The operation of the protection device is not clearly described but the authors probably use a passive crowbar that is triggered when an over-voltage in the dc link occurs, as described in Pourbeik et al. (2003).

Niiranen (2004) presents several topologies for the crowbar circuit, e.g. an antiparallel thyristors crowbar or a half-controlled thyristor-bridge crowbar, as well as a solution based on a diode bridge crowbar. This type of crowbar rectifies the rotor phase currents by means of a diode bridge and uses a controllable thyristor or IGBT to control the shorting, as shown in Figure 9.

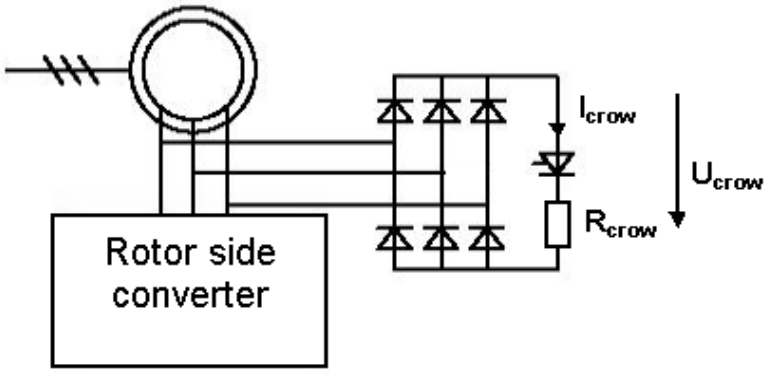

Figure 9. The crowbar connected between the rotor of the DFIG and rotor-side converter.

The crowbar circuit in Figure 9 depicts the concept that was used in this study. The crowbar consists of a diode bridge that rectifies the rotor phase currents and a single thyristor in series with a resistor R_{crow}. The thyristor is turned on when the DC link voltage U_{dc} reaches its maximum value or the rotor current reaches its limit value. Simultaneously, the rotor of the DFIG is disconnected from the rotor-side frequency converter and connected to the crowbar. The rotor remains connected to the crowbar until the main circuit breaker disconnects the stator from the network. When the grid fault is cleared, the rotor-side converter is restarted, and after synchronization, the stator of the DFIG is connected to the network. Rotor over-current protection that operates as described above is called a passive crowbar.

The same circuit topology as shown in Figure 9 is also used in the case of the active crowbar (Niiranen 2004) that was used in the ride-through study (Publication P6). In contrast to a conventional passive crowbar, the active crowbar is fully controllable by means of a semiconductor switch. This type of crowbar is able to cut the short-circuit rotor current whenever needed and thus the DFIG wind turbine is able to ride through a network disturbance. A typical

ride-through sequence (Virtanen 2004) starts when the grid voltage decreases rapidly to a low level. This causes high current transients both in the generator stator and rotor. If either the rotor current or dc link voltage levels exceed their limits, the IGBTs of the rotor-side inverter are blocked and the active crowbar is turned on. The crowbar resistor voltage and dc link voltage are monitored during the operation of the crowbar. When both these voltages are low enough, the crowbar is turned off. After a short delay for the decay of the rotor currents, the rotor-side inverter is restarted and the reactive power is ramped up in order to support the grid.

3.4 Model of the network used for transient performance study

The complexities of the power network model that are used in the transient studies of a DFIG vary from very complex models to rather simple ones. A rather complex grid model, which represents a part of the Danish power grid, is shown in Akhmatov (2006). In Rodríguez et al. (2002), the power networks in several Spanish regions were modeled in order to study the impact of wind power generation on a transmission network.

A simpler network representation is usually used in the case of a wind farm operation study, e.g. Holdsworth et al. (2003b). A generic network model is used for transient performance assessment in Hughes et al. (2005). This model comprises a local network of a wind farm and conventional power generation system connected to the main network through coupling transformers and transmission lines, where a single DFIG represents the aggregated behavior of the individual wind farm generators.

The example of a rather simple model of the power network in Ledesma and Usaola (2001) consists of two transmission lines, a synchronous generator, and a main transformer that couples the DFIG with the main network.

The model of the test set-up network used in this study is depicted in Figure 10. The test set-up was used for the experimental validation of the theoretical results as shown in Publication P4. The scheme consists of a three-phase voltage source model in series with a short-circuit inductance L_{SG} and resistance R_{SG} that represent a simple model of the synchronous generator SG. The time variation of the SG voltage amplitude and frequency was defined in the simulator by look-up table data which were extracted from the measured voltage.

The transmission line between the network and transformer is modeled with its resistance R_{cable} and inductance L_{cable}. A simple linear model represents the main transformer, i.e. magnetic saturation was not taken into account. The transformer model contains a short-circuit resistance R_{TR}, inductance L_{TR}, and the stray capacitance of the winding C_{stray}. The short-circuit resistance R_{SH} and inductance L_{SH} represent another transformer that generates the voltage dip by closing the switch S_{dip}.

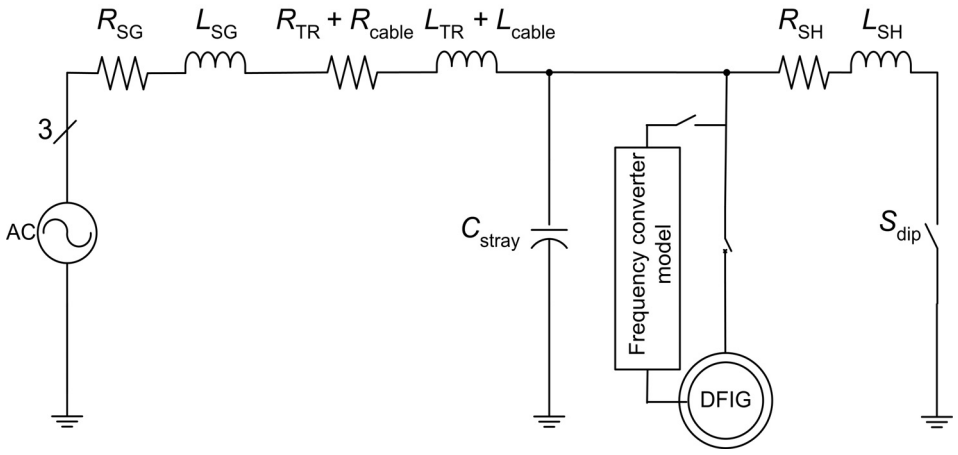

Figure 10. The model of the test set-up network.

4 Modeling of the mechanical part of the wind turbine and its control

The model that represents the mechanical part of the DFIG wind turbine and its control in dynamic studies of power systems usually consists of the following subsystems

- wind speed model
- aerodynamic model
- drive train model
- rotor speed and pitch angle controller.

The complexity of the particular models presented in the literature varies from the very detailed (Akhmatov 2002) to rather simple ones where the rotor speed is considered to be constant (Petersson et al. 2005), depending mainly on the purpose of the study. A detailed literature study, which provides a rather detailed overview of the mechanical modeling of variable-speed wind turbines, is presented in Hokkanen et al. (2004).

The mechanical model and control of the wind turbine was simplified in this study and the rotor speed was considered to be constant except in the comparative study (Publication P5). This study benchmarks detailed and simplified DFIG wind turbine models in order to reveal the influence of the complexity of the mechanical model on transient simulation accuracy during a short-term grid disturbance. The detailed model of the DFIG wind turbine includes a rotor aerodynamic model, wind turbine control, and two mass mechanical drive train models, while the simplified model omits the mechanical model.

4.1 Aerodynamic model of wind turbine

This is basically a wind turbine rotor model for converting the kinetic energy contained in the wind into mechanical power that can be applied to the generator. The speed of the wind is considered to be constant in most of the power system dynamic studies but could also be generated by a wind speed model as presented in Slootweg et al. (2003).

The wind turbine rotor is a complex aerodynamic system and thus a sophisticated method such as e.g. blade element theory (Heier 1998) should be applied. However, this approach is computationally rather demanding and requires detailed information on the wind turbine rotor geometry. In most of the DFIG wind turbine transient and ride-through studies in which the electrical behavior of the system is the main objective, the rotor model is simplified. The simplification is based on the assumption that the mechanical power captured by the wind turbine depends on the power coefficient C_P, which is a function of the tip speed ratio. This type of simplified model is used e.g. by Tapia et al. (2003) and Kana et al. (2001), where the aerodynamic model also includes a tower effect representation.

The aerodynamic model of the wind turbine rotor in Publication P5 is based on the power coefficient C_P look-up table as presented in Iov et al. (2004).

$$T_{wt} = 0.5\pi\rho R^2 v_\infty^3 C_P \tag{4.1}$$

where ρ is the air density, R is the blade radius, v_∞ is the wind speed, and C_P is the power coefficient. As already mentioned, the power coefficient C_P for variable speed wind turbines is a function of the tip speed ratio λ and pitch angle θ, as shown in Figure 11.

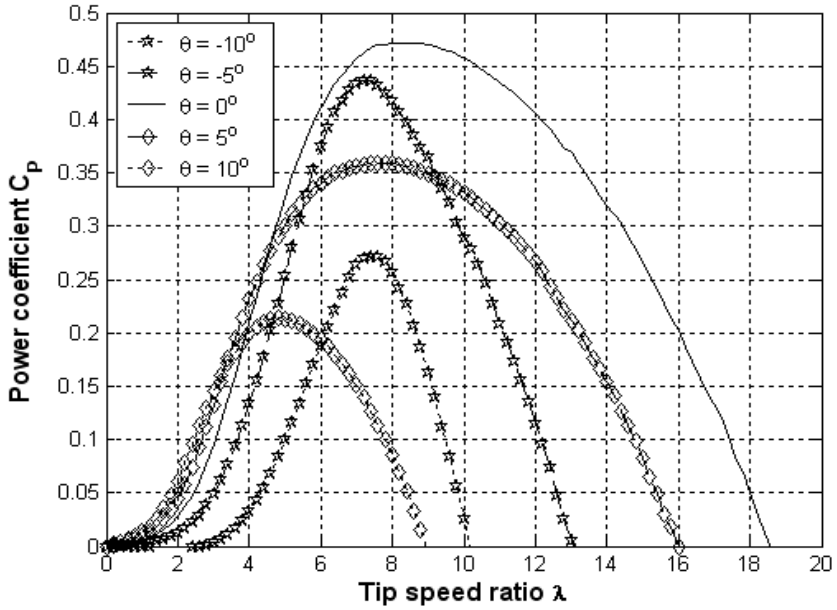

Figure 11. Power coefficient curves for a modern three-blade wind turbine.

For reasons of clarity, the power coefficient is plotted in Figure 11 for a few values of the pitch angle, while the look-up table used in the model contains the power coefficient for the values of the pitch angle from –90° to +90° and tip speed ratio within the range 0 to 20.

The tip speed ratio is defined as

$$\lambda = \frac{\Omega R}{v_\infty} \tag{4.2}$$

where Ω is the rotational speed of the wind turbine.

4.2 Drive train model

The mechanical part of the wind turbine consists of a shaft system and the rotor of the wind turbine itself. Most of the DFIG wind turbine models used in dynamic stability studies include a drive train model. There are two main approaches used for modeling the drive train, the so-called two-mass model (Akhmatov 2002, Ledesma and Usaola 2005), or the frequently used

lumped model approach, which assumes that all the rotating masses can be treated as one concentrated mass (Holdsworth et al. 2003a, Slootweg et al. 2003). The lumped model approach may be insufficient in the case of transient analysis. The impact of the simplification of the drive train model on the accuracy of wind-generator modeling is discussed in Salman and Teo (2003).

The model of a wind turbine drive train is represented in Publication P5 by means of a two-mass model considering an equivalent system with an equivalent stiffness and damping factor on the wind turbine rotor side (Hansen et al. 2003), as shown in Figure 12.

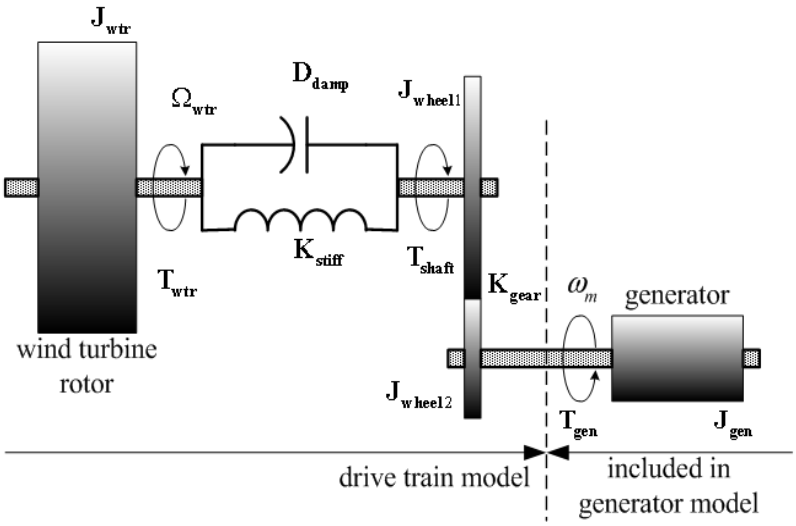

Figure 12. Equivalent model of a wind turbine drive train.

Usually, a one-mass model for the equation of motion is included in the generator model. Therefore, the dynamic equations of the drive train are expressed as

$$\frac{d\theta_k}{dt} = \Omega_{wtr} - \frac{\omega_m}{K_{gear}} \tag{4.3}$$

$$\frac{d\Omega_{wtr}}{dt} = \Omega_{wtr} \tag{4.4}$$

$$\frac{d\theta_{wtr}}{dt} = \frac{1}{J_{wtr}}\left(T_{wtr} - T_{shaft}\right) \tag{4.5}$$

$$T_{shaft} = D_{damp}\Omega_{wtr} - D_{damp}\frac{\omega_m}{K_{gear}} + K_{stiff}\theta_k \tag{4.6}$$

where T_{wtr} - wind turbine torque, J_{wtr} - wind turbine moment of inertia, Ω_{wtr} - wind turbine mechanical speed, K_{stiff} - spring constant indicating the equivalent torsional stiffness of the shaft on the part of the wind turbine, D_{damp} - equivalent damping coefficient of the shaft, T_{gen} - generator torque, J_{gen} - generator moment of inertia, ω_m - generator mechanical speed, K_{gear} - the gearbox ratio, θ_k - angular difference between the two ends of the flexible shaft.

4.3 Wind turbine control

Together, the control system of a variable-speed wind turbine and the induction generator control form the two levels of control, with different bandwidths strongly connected to each other. The main goal of the wind turbine control system is to control the power interchanged between the generator and the grid and to track the optimum wind turbine operation point or to limit the output power in the case of high wind speeds (Hansen et al. 2003 and 2004).

The wind turbine control has slow dynamics compared with the generator control and contains two cross-coupled controllers: a speed controller and a power limitation controller. The control method used in Publication P5 is based on two static optimum curves: the mechanical power of the wind turbine versus wind speed and electrical power versus generator speed, as shown in Figure 13.

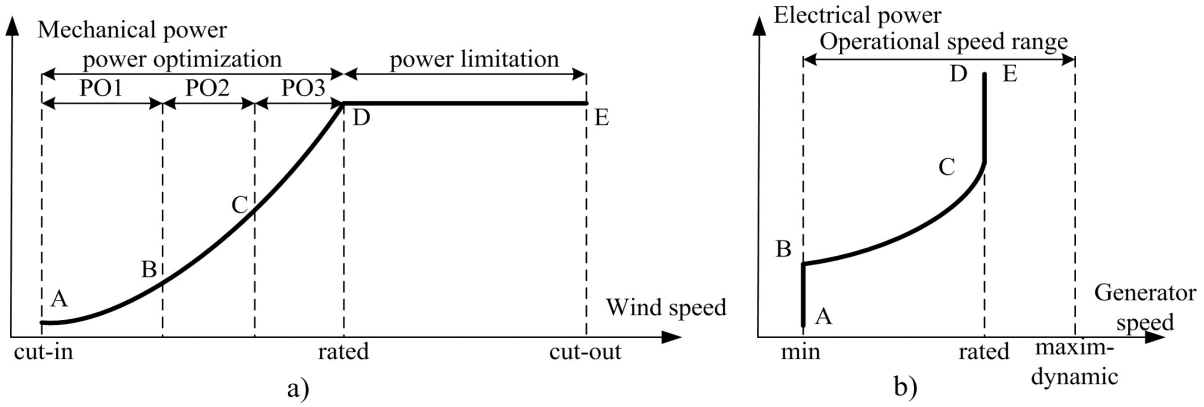

Figure 13. a) Mechanical power versus wind speed and the operation modes for the wind turbine control. b) Electrical power versus generator speed characteristic.

The power optimization strategy and power limitation strategy are the main control strategies used for variable-speed operation. These control strategies are defined in Hansen et al. (2003) and Iov et al. (2003).

The set of two controllers, namely the speed controller and the pitch controller, represent the control system of the variable-speed wind turbine. Since the optimum pitch angle is zero in the power optimization mode, the pitch controller is not active. Therefore, the main controller for this control strategy is the speed controller. In the power limitation mode, both the controllers are active and cross-coupled to each other.

The main tasks for the speed controller is to keep the generator speed at its lower limit for the PO1 strategy, and to adapt the generator speed and therefore to maintain the optimum tip speed ratio for the PO2 strategy. The speed controller also keeps the generator speed at its rated value and allows dynamic variations in a predefined range in the PO3 and power limitation strategy. The structure of this controller is presented in Figure 14a. The reference

torque for the generator control level is obtained from the measured power at the connection point of the wind turbine using the optimum characteristic of the generator speed.

In order to limit the output of the wind turbine to its rated value, the pitch controller has the main task of modifying the pitch angle. The structure of this controller is shown in Figure 14b. The error signal between the measured power P_{grid}^{meas} at the connection point and reference power is P_{grid}^{ref} applied in a PI controller, which produces the reference pitch angle θ^{ref}. This reference is compared with the actual pitch angle θ and the pitching servomechanism corrects the error between these two signals. The model accounts for the time constant of the servomechanism T_{servo} and the limitation of both the pitch angle and its gradient so that a realistic response of the control system is obtained.

As there is a non-linear relation between the pitch angle and the wind speed, a non-linear control, so-called gain scheduling, is used. Instabilities would be obtained at high wind speeds if a linear control was used. More details of gain scheduling and its impact on the stability of the control loop are presented in Hansen et al. (2004).

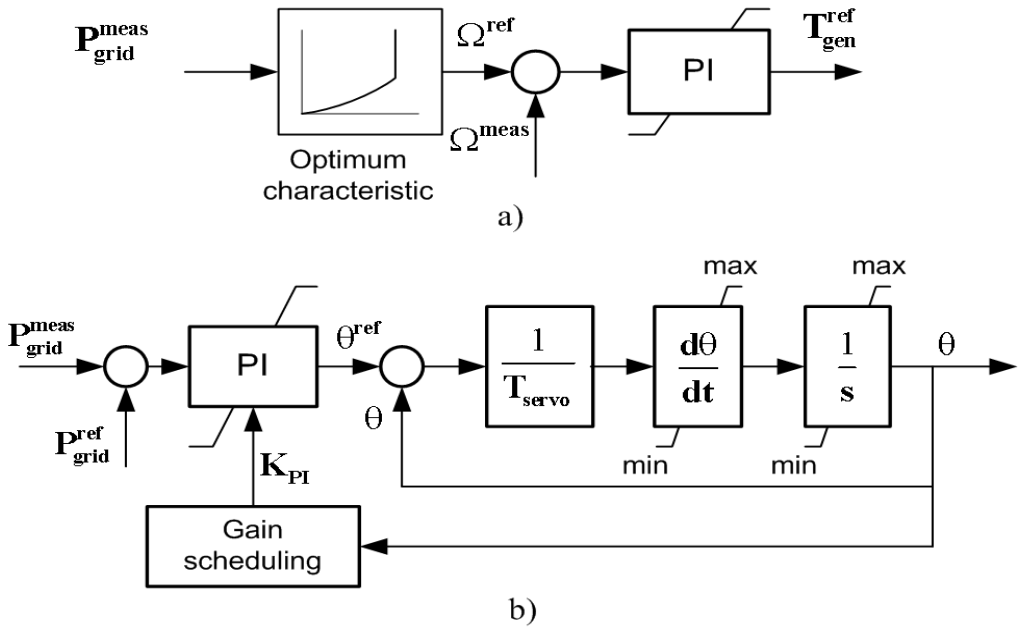

Figure 14. a) Structure of the speed controller for a DFIG wind turbine. b) Structure of the pitch controller for a DFIG wind turbine.

5 Transient and ride-through analysis

Because of the ongoing trend of there being significant penetration of wind-power generation systems into power networks world-wide, it is necessary to study the interaction between wind-power generators and power networks, especially the operation of wind-power generators during grid disturbances. Various power system operators are nowadays revising their grid codes to ensure that wind turbines can continue their operation for a certain time period in the event of a grid fault. According to the requirements presented in the proposals for the new grid codes, e.g. E.ON Netz (2003), during a grid fault wind turbines should be able to control their voltage and frequency and stay connected to the power network so as to prevent the power system from collapsing. This capability is commonly known as ride-through capability (Salman et al. 2004).

5.1 Grid codes

Grid codes define the responsibility of the wind turbine owner for wind turbines connected to a power grid to meet the technical regulations of the power system operator. Grid codes also specify the responsibilities of the owner of the wind turbine to protect it against damage caused by internal or external impacts, active and reactive power control, frequency control, voltage quality, and the external control of the wind turbine (Eltra 2004a). Significant attention is paid to the interaction between the wind turbine and the rest of the power system during grid faults and to the testing methods used in the verification of the ride-through capability of the wind turbine.

The Danish system operator specifies the grid code requirements separately for Wind Turbines Connected to Grids with Voltages below 100 kV (Eltra 2004a) and above 100 kV (Eltra 2004b), which also specifies wind farms' stability in the event of asymmetric grid faults and unsuccessful re-closure.

The Scottish grid code (SB/2 2002) requires a wind turbine with a non-synchronous generator to remain connected to the grid in the event of a zero-voltage grid fault for 140 ms.

The transmission utility from Germany, E.ON Netz, specifies the requirements for wind turbines connected to transmission networks of 110 kV or above. The grid code regulations (E.ON Netz 2003) were considered in this study, especially in Publication P6. This grid code states that wind turbines must not be disconnected from the network in the event of an 85% voltage dip caused by a three-phase short circuit for 150 ms with voltage recovery to 80% within 3 seconds, as shown in the voltage-limiting curve in Figure 15. Active power output must resume immediately after the clearing of the fault and be ramped up with a gradient of at least 20% of the rated power per second. Within the shaded area in Figure 15, the active power increase can take place at 5% of the rated power. In addition to the above mentioned

requirements, support of the network must be provided within 20 ms after identification of the fault by providing reactive power at the generator terminals with a factor of 2% of the rated current per percent of voltage drop.

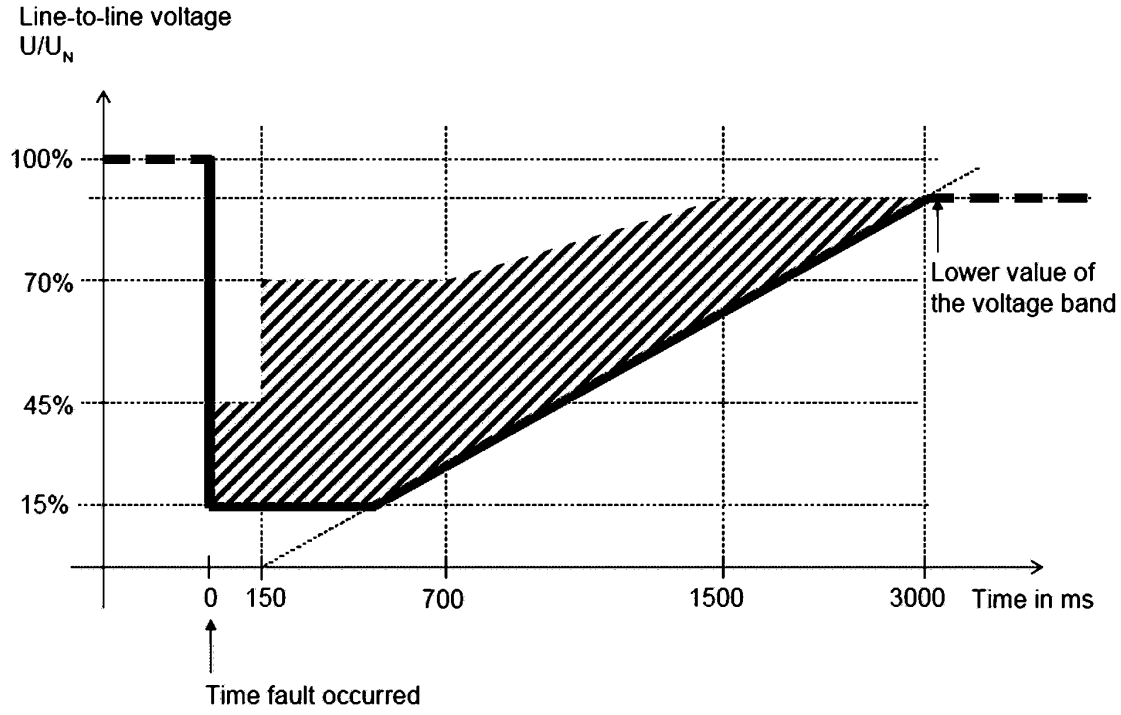

Figure 15. The voltage-limiting curve at the network connection above which generating units must not be disconnected (E.ON Netz 2003).

It could be concluded that the main goal of the grid code specifications is to define the control of the DFIG in such a way that it will behave in the same way as a conventional synchronous generator from the grid integration point of view.

5.2 Transient and ride-through analysis of DFIG wind turbines under a grid fault

The transient simulations presented in the literature are performed on different levels of accuracy and we can also recognize two main groups of simulation analysis:

- Transient stability analysis
- Short-term voltage disturbance transient and ride-through analysis.

The models developed for transient stability analyses (Holdsworth et al. 2003a, Slootweg et al. 2003, Ekanayake and Jenkins 2004, Choudhury and Chellapilla 2005) are generally valid in longer time frames. These studies are focused on the interaction of DFIG turbines or wind farms with power grids in slower transient conditions, such as the potential for voltage flicker, power oscillations caused by wind speed variation, gusts, ramp etc. Simplified models of the

DFIG and converters are frequently used to make it possible to use long integration steps in order to make them suitable for implementation into complex power system simulators.

The simulation models of DFIG wind turbines used for short-term voltage disturbance transient analyses (Akhmatov 2002, Ekanayake et al. 2003b, Thiringer et al. 2003) and ride-through analyses (Niiranen 2004, Hogdahl and Nielsen 2005, Morren and de Haan 2005) are usually rather different compared to the stability transient models. These studies include very fast transients, e.g. grid disturbances such as lightning, or switching surges, where lightning causes the majority of the grid faults surges (Salman et al. 2003). Simulating fast transient phenomena requires the use of a small integration time step for the numerical integration and also more complex and detailed models of the generator and power electronics, as discussed in Koseller et al. (2003). The use of small time steps and complex transient models results in longer simulation times in comparison with the transient stability analyses.

The grid codes presented in the previous sub-chapter recognize transient simulation as one of the testing methods that can be used for the approval testing of wind turbine power production capability during and after a grid fault (Eltra 2003). Most grid codes require the simulation of the symmetrical 3-phase short circuit in order to investigate wind turbine behavior in the event of a grid fault. The newer grid codes, for example Eltra (2005), also prescribe the carrying out of a simulation test that will verify the capability of the wind turbine to withstand the impact of asymmetrical faults. The simulation test is usually performed at a wind velocity that results in the production of the rated power with full compensation and voltage at the generator terminals.

Most of the papers study the transient behavior of the DFIG under a 3-phase short-circuit fault, as presented in e.g. Ekanayake et al. (2003b), Pöller (2003), Niiranen (2004) and Salman and Teo (2003). The transient behavior of DFIG wind turbines during asymmetrical faults has been studied by simulation in Lund et al. (2005) and experimentally in Piekutowski et al. (2005).

A significant part of the material included in this work (Publications P1-P5) is dedicated to the short-term analysis of a 1.7-MW DFIG wind generator under a symmetrical 3-phase grid fault. The ride-through analysis of the same DFIG wind generator under an unbalanced grid fault is presented in Publication P6.

6 Experimental set-up

The majority of the transient and ride-through analysis results presented in the literature were obtained by theoretical investigations that were carried out by means of numerical simulation. These studies mainly come from the academic environment and it is evident that experimental verification of the simulation results by means of a full-scale test is usually not possible at universities.

In order to solve this problem, some low-power laboratory test set-ups have been built. The low-power laboratory test set-up presented in Tang and Xu (1995) is used for the verification of the functionality of the proposed control algorithm, Brune et al. (1994) examine the steady-state performance of the wind generator, and Vicatos and Tegopoulos (1991) experimentally verify DFIG transient performance during a short circuit.

On the other hand, the contributors from industry present the experimental results of full-power tests that have been performed in order to verify the transient and ride-through simulation results (Rodrígues et al. 2002, Hogdahl and Nielsen 2005, Niiranen 2005, Piekutowski et al. 2005). Recently, a few studies have also been presented that are based on collaboration between universities and industry, in which full-power tests were carried out using industrial test facilities in order to validate the simulation results, e.g. Peterssen et al. (2005), Publication P4.

Full-scale measurements verified the transient simulation study results of the DFIG wind power generator and validated the coupled field-circuit simulator (Publication P4). The set-up shown in Figure 16 consisted of a wind-power DFIG and frequency converter that are used for variable-speed 2 MW wind turbines, a large synchronous generator acting as a grid, and two transformers.

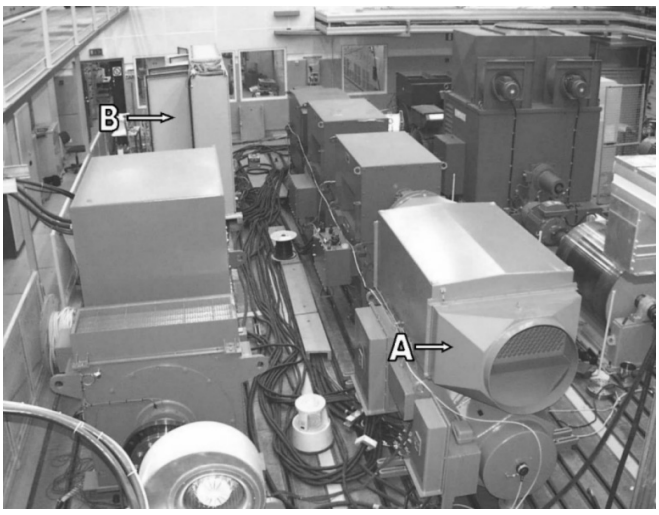

Figure 16. Photograph of a part of the test set-up at the ABB test laboratory. DFIG, marked "A", is on the right. The frequency converter is the cabinet marked "B" on the left.

The generator was powered by a prime mover at a constant speed instead of a 2 MW wind turbine. These tests were performed at the ABB Oy Finland test facilities, as it was not possible to conduct field tests on a 2 MW wind turbine during a grid fault.

A single line diagram of the full-scale measurement set-up is shown in Figure 17. The set-up consists of a 1.7-MW DFIG with frequency converter, a large synchronous generator SG acting as a grid, and two transformers. A DFIG with a stator current rating of 1600 A can be loaded to generate more than 2 MW when run at maximum super-synchronous speed. The transformer TR 1 transforms the synchronous generator output voltage 11.5 kV to the 690 V that is the voltage level of the doubly fed equipment. The other transformer TR 2 is used as a short-circuit impedance.

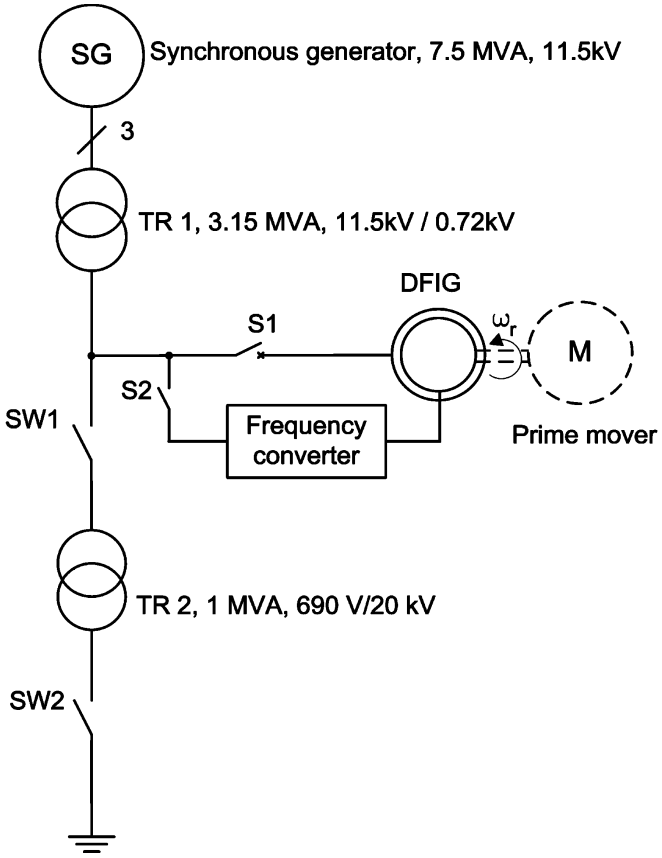

Figure 17. Schematic diagram of the test set-up.

At the beginning of the test the circuit breaker SW1 is closed and SW2 is open. Closing the circuit breaker SW2 in the transformer's secondary generates the voltage dip and opening the circuit breaker SW1 terminates the voltage dip.

The equivalent circuit of the test set-up was described in Chapter 3.4, Model of the network used for transient performance study. The rated parameters of the DFIG are given in Table 6.1 and the test set-up network parameters are given in Table 6.2.

Table 6.1. The rated parameters of the DFIG

P_N	*rated power*	*1.7 MW*
U_N	*rated stator voltage*	*690 V (delta)*
I_N	*rated stator current*	*1600 A*
$U_{max,r}$	*maximum rotor voltage* [1]	*2472 (star)*
f_N	*rated stator frequency*	*50 Hz*
n_N	*nominal speed*	*1500 rpm*

[1] *In normal use rotor voltage is proportional to slip.*

Table 6.2. The network parameters of the test set-up

DFIG star equivalent circuit parameters (resistances at 20°C temperature, reactances at 50-Hz frequency)	
R_s	1.615 mΩ
$X_{s\sigma}$	28.83 mΩ
X_m	787.8 mΩ
R_r'	2.369 mΩ
$X_{r\sigma}'$	25.77 mΩ
TR 1 equivalent circuit parameters	
X_{TR}	9.07 mΩ
R_{TR}	1.51 mΩ
TR 2 equivalent circuit parameters	
X_{SH}	29.5 mΩ
R_{SH}	4.76 mΩ
Parameters of a synchronous generator equivalent L-R model based on the transient impedance	
X_{SG}	29.5 mΩ
R_{SG}	4.76 mΩ
Parameters of an L-R model of 690-V cable	
X_{cable}	11 mΩ
R_{cable}	15 mΩ

7 Discussion of the results

A new coupled field-circuit simulator based on an indirect-coupling methodology for combining FEM computation with Simulink was developed. The field-circuit simulator combines the accuracy of FEM computation with the flexibility of the commercial system simulator and also makes it possible to observe in detail the influence of the operation of the frequency converter on an electrical machine. The proposed simulator was verified for the first time by a simulation study of an induction motor fed by a DTC-controlled frequency converter under the transients presented in Kanerva et al. (2003).

A new method for coupling the magnetic field equations with circuit equations was developed and benchmarked with a directly coupled field-circuit simulation technique in Publication P3. The comparison of the simulation results obtained from the simulation of a doubly fed induction generator in steady state and a three-phase short circuit shows good agreement between both the methods. However, the newly-developed method exhibits some drawbacks, such as a slightly higher time consumption and possible numerical instability without additional filtering (Kanerva 2005). The method is the most beneficial in those cases where the external circuit is relatively complex and consists mostly of passive circuit elements. For plain impedance in series with the windings, direct coupling with FEM equations is a simpler approach and thus was used in further analyses of the wind turbine with DFIG.

The only study found in the literature on DFIG wind power generator performance analysis when the coupled field-circuit approach is used was presented in Runcos et al. (2004). This study, however, analyses a brushless doubly fed induction generator modeled by the FEM and coupled with a very simple frequency converter representation, with no detailed control algorithm of the wind-power conversion system included. The paper focuses mainly on the operational and design aspects of the electrical machine.

The transient behavior and ride-through capability of a 1.7-MW wind-power generator equipped with a DFIG under a network disturbance was studied in Publication P1. The DFIG was supplied to the rotor from a modified direct torque-controlled and crowbar-protected frequency converter.

The implementation of a DTC for variable speed wind turbines with a DFIG was presented by Arnalte et al. (2002). This work, however, evaluates only the suitability of the DTC control scheme for use for the active and reactive power control of a DFIG wind turbine as an alternative to the widely used field-oriented control scheme (Pena et al. 1996).

Comparison of the transient behavior of a 1.7-MW DFIG under a three-phase network short circuit with and without the crowbar reveals the importance of the implementation of the crowbar in order to protect the rotor-side converter and rotor circuit of the DFIG during a grid fault. When the passive crowbar is implemented, the stator and rotor transient currents decay

rapidly to values with an amplitude lower than 1 p.u., as depicted in Figure 18, in contrast with the case when the crowbar is not implemented, as illustrated in Figure 19. The simulation results also show that the amplitude of the transient electromagnetic torque is reduced when the crowbar is activated.

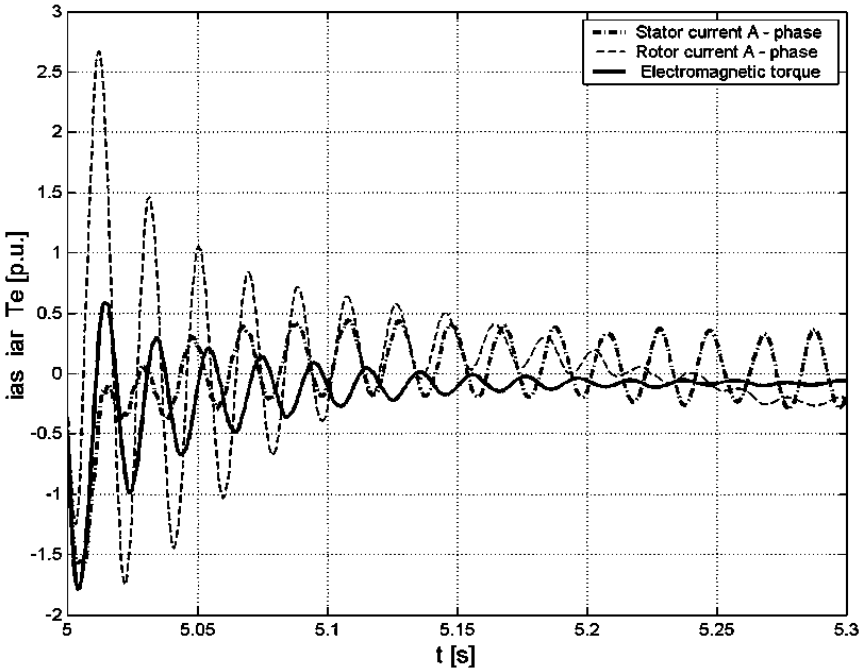

Figure 18. Stator current (dash dot), rotor current (dash), and electromagnetic torque (solid) during network disturbance with the crowbar implemented.

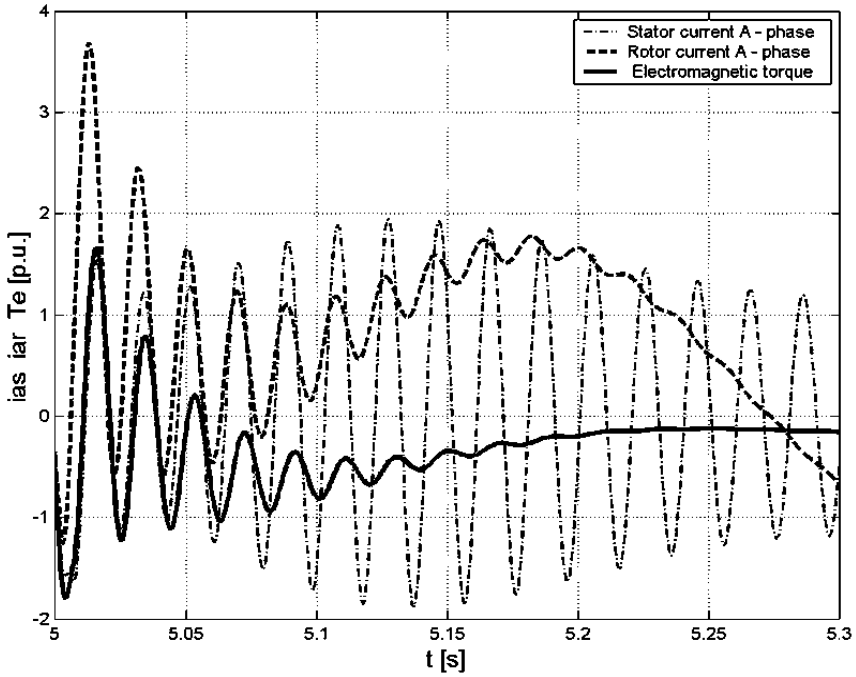

Figure 19. Stator current (dash dot), rotor current (dash), and electromagnetic torque (solid) during network disturbance without the crowbar implemented.

The simulation study of the DFIG wind-power generator under a grid disturbance presented in Publication P2 benchmarks the coupled field-circuit simulator and simulator based on an analytical model. This study shows that the transient currents and electromagnetic torque obtained from the FEM model have higher peak values at the beginning of the transient in comparison with the analytical model. This is mainly due to the effect of magnetic saturation on the stator and rotor leakage inductances, which is taken into account in the FEM.

Most of the model comparative studies presented in the literature compare third-order simplified DFIG models with fifth-order models, focusing on their suitability for use in short-term transient analysis (Ekanayake et al. 2003a, Ledesma and Usaola 2003). The authors conclude that the third-order model is sufficient to represent the DFIG even in the short term and it is not necessary to use the fifth-order model. This is, however, in contrast with the conclusions of the more experimentally-oriented group, for example Akhmatov (2003) or Koessler et al. (2003). They state that the third-order model should be used for transient stability studies and the short-term grid disturbance transient analysis should be carried out by means of more detailed fifth-order models that will accurately represent the non-linearities, dc components, and unbalanced operation. Taking into account this consideration, a detailed field-circuit model of a DFIG wind turbine was developed and used in short-term transient analysis. The comparison of the simulation results in Publication P2 proves that the more detailed FEM model can model the transient behavior of the DFIG under a short-term grid disturbance more accurately than the traditional analytical model.

The full-power transient measurements on the test set-up with a 1.7 MW doubly fed wind-power generator were carried out in order to verify the simulation results (Publication P4).

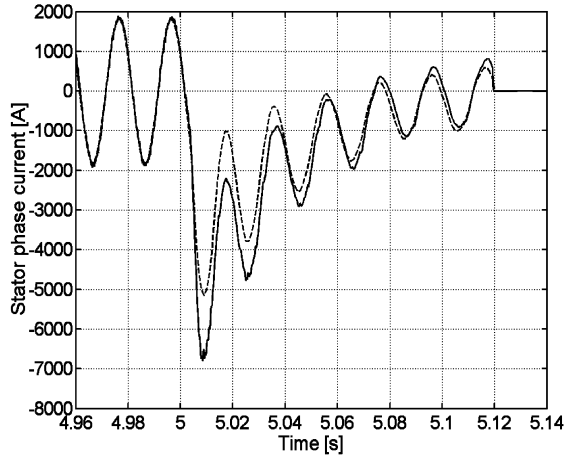

Figure 20. The transient stator current obtained from the FEM model (solid) and transient stator current obtained by the analytical model (dashed).

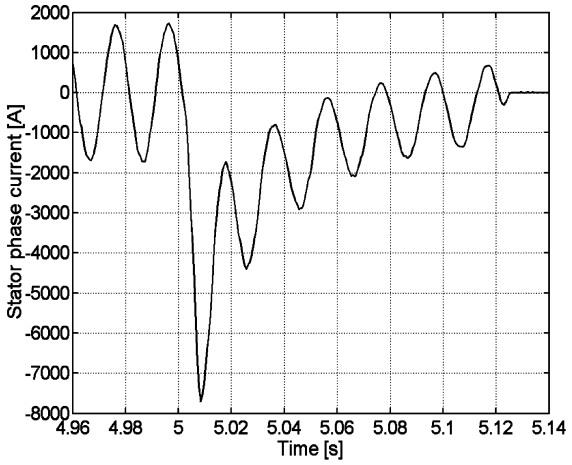

Figure 21. The measured transient stator current.

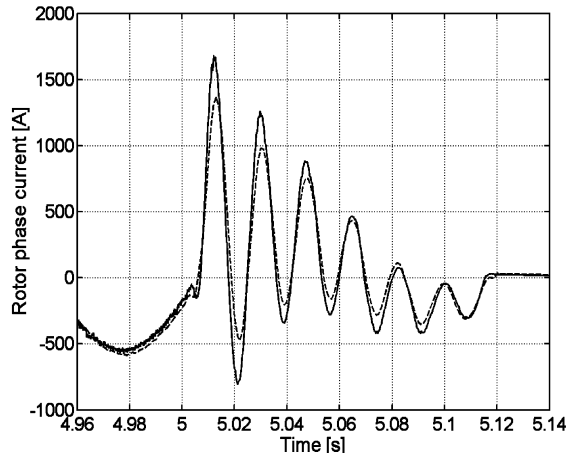

Figure 22. The transient rotor current obtained from the FEM model (solid) and transient rotor current obtained by the analytical model (dashed).

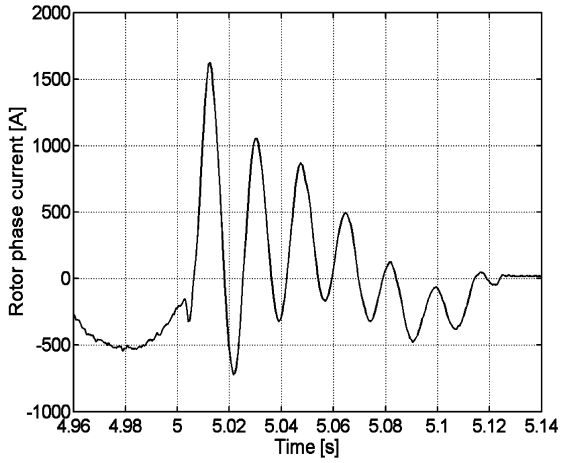

Figure 23. The measured transient rotor current.

The simulation results obtained by means of the coupled FEM circuit simulator presented in Figures 20 and 22 show good agreement with the experimental results in Figures 21 and 23, especially at the beginning of the transient, while the analytical model manifests certain drawbacks. This is due to the fact that the magnetic saturation is taken into account in the FEM, whereas in the analytical model the lumped parameters are considered to be constant. The coupled FEM circuit model gives a more realistic view of the maximum currents in the stator and rotor during a grid disturbance than the analytical model.

Experimental validations of the simulation analysis performed with a full-scale laboratory set-up are presented in Niiranen (2004 and 2005) or directly on the wind turbine in Hogdahl and Nielsen (2005) and Petersson et al. (2005). The experimental results in Petersson et al. (2005) were obtained from the measurements on a "fictitious" 850 kW DFIG wind turbine, which probably means that the control of the frequency converter, as well as the details regarding the wind turbine control and DFIG, were not known exactly. The paper analyzes shallow voltage dips introduced to the DFIG wind turbine by means of a simulator based on a third- and fifth-order induction generator model and compares the simulations with measurements. Here, the authors state rather good agreement between the simulation and experimental results; however, these conclusions are not convincing because the simulated system, e.g. the frequency converter control and crowbar operation, is not exactly defined in the paper. The experimental results obtained from a severe voltage disturbance represented by a voltage dip of approximately 60% are not compared with the term grid disturbance and using the simplified model would probably not help to obtain realistic results.

The results of the simulation analysis and full-power test in Publication P4 demonstrate that the analytical models are not sufficient for the accurate transient analysis of DFIG under a short-term grid disturbance and using the simplified model would probably not help to obtain realistic results.

The three variable-speed wind turbine simulators used for the short-term transient behavior analysis of a 2 MW wind turbine were compared in Publication P5, showing the influence of the different modeling approaches on the accuracy of the short-term transient simulation.

Studies focused on the transient behavior of a DFIG under a grid fault usually consider the representation of the shaft system by means of a simplified one-mass model with a so-called lumped moment of inertia (Ekanayake et al. 2003b) or by an advanced two-mass model (Ledesma and Usaola 2005). A study of wind turbine drive train modeling which compares the one-mass and two-mass models from the point of view of the dynamic behavior investigation accuracy of a DFIG wind farm is presented in Salman and Teo (2003). The importance of the model representation of the drive train in short-term voltage stability investigations is discussed in Akhmatov (2003). The author recommends using the two-mass model in cases of low shaft stiffness, and, in cases where the shaft is relatively stiff, the model can be reduced to a lumped one-mass model.

On the other hand, the comparison of the simulation and experimental analysis performed on a Vestas V80 VCS wind turbine by Hogdahl and Nielsen (2005) shows that the influence of the turbine speed behavior on the ride-through is small. A similar fact was observed in the comparative simulation study in Publication P5. The comparison of the transient rotor currents is depicted in Figure 24. The frequency of the rotor current calculated by the DFIG wind turbine simulator varies as a result of variations in rotor speed. The difference in frequency is clearly visible before the transient. At the beginning and at the end of the transient, some small differences in the amplitudes of the compared rotor currents can be observed. Figure 25 shows the variation of the rotor speed and also compares the active and reactive power of the generator during the transient. A slight difference between the results can be observed at the end of the transient. simulation results.

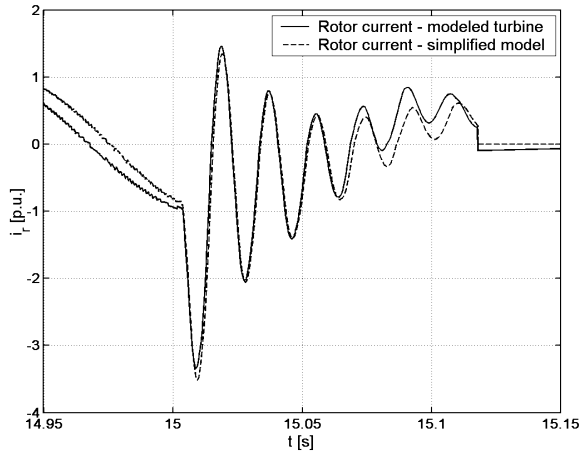

Figure 24. The rotor current obtained from the detailed turbine model (solid) and from the simplified model (dashed) during a grid disturbance.

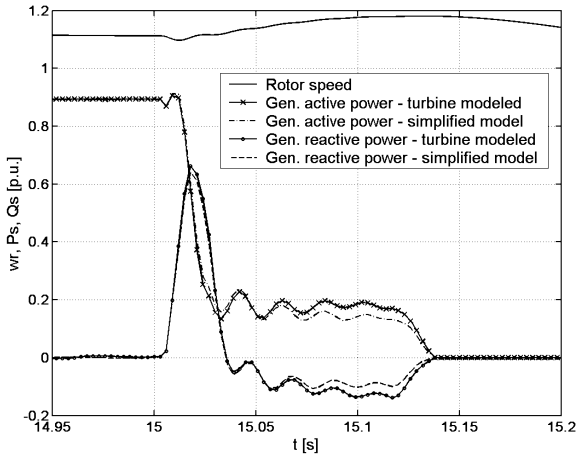

Figure 25. The rotor speed (solid) active power from the detailed model (solid "x") and the simplified model (dash-dot), reactive power from the detailed model (solid "o") and from the simplified model (dashed) during a grid fault.

It can be concluded that the representation of the shaft system could be omitted in short-term transient behavior and ride-through studies of DFIG wind turbines without a significant impact on the accuracy of the transient simulation. The accuracy of the transient simulation could, however, be significantly improved by the detailed modeling of the induction generator, as has already been discussed.

The ride-through simulation study of a 2 MW wind-power DFIG during a short-term asymmetrical network disturbance was performed in order to show the ride-through capability of the studied wind power generator (Publication 6). Differences in the simulation results of the DFIG were observed, especially when a grid fault was introduced. The comparison of the simulated electromagnetic torque obtained by the FEM and the analytical model exhibits a large difference at the beginning of the transient that is mainly caused by the fact that the FEM model represents the asymmetrical magnetic saturation better than the conventional analytical model.

In addition to the results presented in Publication P6, the positive and negative sequence stator phase current and voltage were calculated in order to compare the results obtained by the different simulation approaches. The positive sequence quantities are used in one of the methods proposed for the calculation of active and reactive power in the event of an unbalanced grid disturbance (Niiranen 2006). Figures 26 and 27 depict the RMS values of the positive and negative sequence phase voltages during the asymmetrical voltage dip studied in Publication P6. Figure 28 compares the RMS values of the positive sequence phase currents obtained from the FEM model and analytical model. The comparison shows that the positive current component calculated by the FEM is typically a little higher than the current component obtained from the analytical model. However, within the time interval 5.05-5.3 s the FEM positive sequence current is smaller than the current from the analytical model and the difference is about 0.1 p.u. During this time interval, the DFIG mainly behaves as a three-phase inductor because of the disconnection of the rotor supply; however, the free-wheel diodes are modeled and cause some peaks in the rotor voltage. Figure 29 compares the RMS values of the negative sequence phase currents. In this case, the negative current component calculated by the FEM is always a little higher than the current component obtained from the analytical model.

No similar ride-through study of a DFIG wind-power generator under an unbalanced grid disturbance has been found in the literature. There are ride-through studies analyzing the transient behavior of the DFIG under a balanced three-phase fault (Niiranen 2004 and 2005, Hogdahl and Nielsen 2005), presented by authors from an industrial background, in which the simulated results are validated by measurements. The paper of Morren and de Haan (2005) presents a ride-through analysis of DFIG wind turbine performance during a grid fault represented by an 85% voltage dip. The authors state that they also take into consideration the requirements defined in E.ON Netz (2003), including the requirement to supply reactive power into the grid during long-term dips, as also considered in Publication P6. However, the fact that

the frequency converter modeling in Morren and de Haan (2005) is not detailed and converters are assumed to be ideal (Morren et al. 2003) does not inspire much confidence in the accuracy of the simulation results. The inclusion of a realistic frequency converter model is one of the key issues that significantly influences the short-term voltage disturbance or accuracy of ride-through analysis, as concluded in Akhmatov (2003) and also in this work. The model of the frequency converter in Publication P6 is a compromise in which the rotor-side frequency converter is modeled in detail and the network-side converter model is simplified. On the basis of the conclusions in Akhmatov (2003), the inclusion of a detailed model of the network-side converter that included the converter control and switching dynamics could probably increase the accuracy of the simulation.

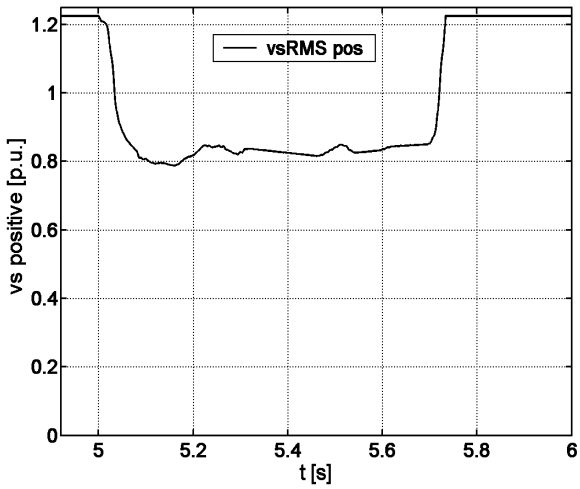

Figure 26. The RMS value of the positive sequence phase voltage.

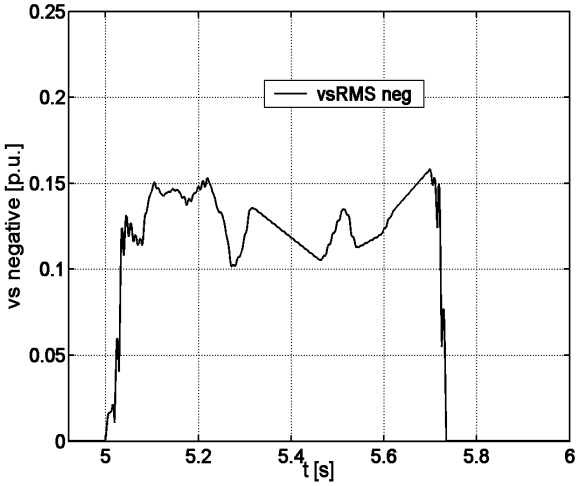

Figure 27. The RMS value of the negative sequence phase voltage

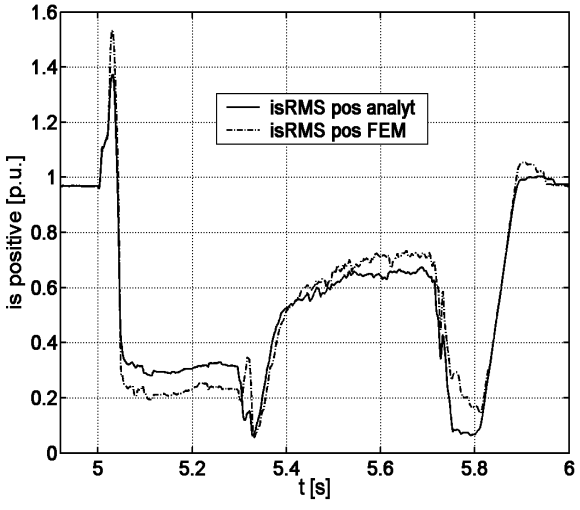

Figure 28. The RMS values of the positive sequence phase current obtained from the FEM model (dashed) and analytical model (solid).

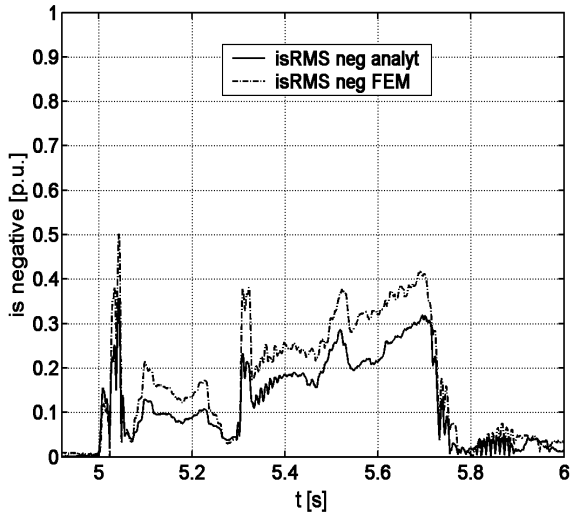

Figure 29. The RMS values of the negative sequence phase current obtained from the FEM model (dashed) and analytical model (solid).

8 Conclusions

The aim of this research was to develop and experimentally validate a coupled field-circuit transient simulator. The developed simulator was then used for the transient analysis of a wind energy conversion system with a doubly fed induction generator. The short-term voltage disturbance analyses and the ride-through analysis of a 1.7 MW DFIG wind-power conversion system under a network disturbance were carried out. Several modeling approaches are compared in order to reveal the consequences of the different modeling approaches for the accuracy of the transient analysis. A 1.7 MW full-scale measurement set-up experimentally validated the coupled field-circuit wind turbine simulator. The impact of the detailed modeling of the DFIG wind turbine on the accuracy of the electrical system performance analysis at the event of a short-term voltage disturbance was also studied.

It has been found that:

1. The FEM calculation can be run simultaneously with the time-stepping simulation of the feeding converter and the interaction between the machine, converter, and control system can be taken into account.

2. It is important to implement a crowbar to the DFIG wind power generator in order to efficiently protect the rotor-side converter and rotor circuits of the DFIG during a grid fault and a grid fault ride-through.

3. The transient currents and electromagnetic torque obtained from the FEM model of the DFIG have higher peak values at the beginning of the transient in comparison with the analytical model. This is mainly due to the effect of magnetic saturation of the stator and rotor leakage inductances, which is taken into account in the FEM.

4. The comparison between the simulated results obtained by means of the coupled field-circuit simulator and full-scale measurement shows reasonable agreement. The analytical model of the DFIG manifests certain drawbacks that are overcome by using a FEM model.

5. The shaft system representation can be omitted in short-term transient behavior and ride-through studies of the DFIG without a significant impact on the transient simulation accuracy, which can, however, be significantly improved by the detailed modeling of the induction generator and frequency converter.

6. The modeled wind-power DFIG is capable of ride-through and it is possible to supply reactive power into the grid during voltage dips. The comparison of different modeling approaches shows that during an asymmetrical fault the FEM model represents the asymmetrical magnetic saturation better, while the conventional analytical model neglects asymmetries.

The developed coupled field-circuit-based simulator has proved to be capable and reliable for modeling complicated power electronics and electrical machine set-ups and thus is a useful tool for the development and optimization of wind-power generators.

References

Abbey, C., Joos, G. 2004. "A Doubly-Fed Induction Machine And Energy Storage System for Wind Power Generation", *Canadian Conference on Electrical and Computer Engineering 2004*, 2-5 May 2004, Vol. 2, pp. 1059-1062.

Abolhassani, M.T., Toliyat, H.A. Enjeti, P. 2003. "Stator Flux Oriented Control of an Integrated Alternator/Active Filter for Wind Power Applications", *IEMDC'03 IEEE International Electric Machines and Drives Conference*, 1-4 June 2003, Vol. 1, pp. 461-467.

Akhmatov, V. 2002. "Modelling of Variable-Speed Wind Turbines with Doubly-Fed Induction Generators in Short Term Stability Investigations", *Int. Workshop on Transmission Networks for Offshore Wind Farms*, 2002, Stockholm, Sweden, 23 p.

Akhmatov, V. 2003. "Analysis of Dynamic Behaviour of Electric Power System with Large Amount of Wind Power", PhD Thesis, Electric Power Engeneering, Orsted DTU Technical University of Denmark, April 2003, Kgs. Lyngby, Denmark, 261 p.

Akhmatov, V. 2006. "System Stability of Large Wind Power Networks: A Danish Study Case", *International Journal of Electrical Power & Energy Systems*, Vol. 28, Issue 1, January 2006, pp. 48-57.

Arkkio, A. 1987. "Analysis of Induction Motors Based on The Numerical Solution Of The Magnetic Field And Circuit Equations", Electrical Engeneering Series No. 59, Acta Polytechnica Scandinavica, Helsinki, Finland, 97 p., Available: http://lib.hut.fi/Diss/198X/isbn951226076X/ (7.5.2006).

Arnalte, S., Burgos, J.C., Rodrigues-Amenedo, J.L. 2002. "Direct torque control of a doubly-fed induction generator for variable speed wind turbines", *Electric Power Components and Systems*, Vol. 30, 2002, pp. 199-216.

Brune, C.S., Spee, R., Wallace, A.K. 1994. "Experimental Evaluation of A Variable-Speed, Doubly-Fed Wind-Power Generation System", *IEEE Transactions on Industry Applications*, Vol. 30, Issue 3, May-June 1994, pp. 648-655.

Chellapilla, S.R., Chowdhury, B.H. 2003. "A Dynamic Model of Induction Generators for Wind Power Studies", *IEEE Power Engineering Society General Meeting*, Vol. 4, 13-17 July 2003, pp. 2340-2344.

Chowdhury, B.H. and Chellapilla, S. 2006. "Double-Fed Induction Generator Control for Variable Speed Wind Power Generation", *Electric Power Systems Research*, Vol. 76, Issues 9-10, June 2006, pp. 786-800.

E.ON. Netz 2003. "Grid Code for High and Extra High Voltage", E.ON. Netz. GmbH, Bayreuth, Germany, August 2003, 51 p., Available http://www.eon-netz.com/Ressources/downloads/enenarhseng1.pdf, (7.5.2006).

Eltra. 2004a. “Wind Turbines Connected to Grids with Voltages Below 100 kV - Technical regulation for the properties and regulation of the wind turbines”, TF 3.2.6, May 19, 2004, 41 p., Available: http://www.eltra.dk (7.5.2006).

Eltra. 2004b. “Wind Turbines Connected to Grids with Voltages above 100 kV - Technical regulation for the properties and regulation of the wind turbines”, TF 3.2.5, December 3, 2004, 34 p., Available: http://www.eltra.dk (7.5.2006).

Ekanayake, J.B., Holdsworth, L., Jenkins, N. 2003a. “Comparison of 5th Order and 3rd Order Machine Models for Doubly Fed Induction Generator (DFIG) Wind Turbines”, *Electric Power Systems Research*, Volume 67, Issue 3, December 2003, pp. 207-215.

Ekanayake, J.B., Holdsworth, L., Wu, X.G., Jenkins, N. 2003b. “Dynamic Modeling of Doubly Fed Induction Generator Wind Turbines”, *IEEE Transaction on Power Systems*, Vol. 18, Issue 2, May 2003, pp. 803-809.

Ekanayake, J. and Jenkins, N. 2004. “Comparison of the Response of Doubly Fed and Fixed-Speed Induction Generator Wind Turbines to Changes in Network Frequency”, *IEEE Transactions on Energy Conversion*, Vol. 19, Issue 4, Dec. 2004, pp. 800-802.

Gokhale K.P., Krakker D.W., Heikkilä S.J. 2004. “Controller for A Wound Rotor Slip Ring Induction Machine”, U.S. Patent 6741059, Available http://patft.uspto.gov (7.5.2006).

Gómez, S.A., Amenedo, J.L.R. 2002. “Grid Synchronisation of Doubly Fed Induction Generators Using Direct Torque Control”, *IEEE 2002 28th Annual Conference of the Industrial Electronics Society IECON 02*, Vol. 4, 5-8 Nov. 2002, pp. 3338-3343.

Hansen A.D., Jauch, C., Sørensen, P., Iov, F., Blaabjerg, F. 2003. “Dynamic Wind Turbine Models in Power System Simulation Tool”, Report, Risø-R-1400, ISBN 87-550-3198-6, 80 p.

Hansen, A.D., Sørensen, P., Iov, F., Blaabjerg, F. 2004. “Control of Variable Pitch/Variable Speed Wind Turbine with Doubly Fed Induction Generator”, *Journal of Wind Engineering*, Vol. 28, No.4, 2004, pp. 411-432.

Heier, S., 1998. “Grid Integration of Wind Energy Conversion Systems”, Willey, Chicester, U.K. 1998.

Hinkkanen. M., 2004. “Flux Estimators for Speed-Sensorless Induction Motor Drives”, Doctoral thesis, Helsinki University of Technology Institute of Intelligent Power Electronics-Publication 9, Espoo, 2004. 46 p., Available: http://lib.tkk.fi/Diss/2004/isbn9512271893/ (7.5. 2006).

Hogdahl, M., Nielsen, J. G. 2005. “Modeling of the Vestas V80 VCS Wind Turbine with Low Voltage Ride-Through”, *Proceedings of Fifth International Workshop on Large-Scale Integration of Wind Power and Transmission Networks for Offshore Wind Farms*, April 7-8, 2005, Glasgow, Scotland, pp. 292-304.

Hokkanen, M., Salminen H. J., Vekara, T. 2004. "A Short Review of Models for Double-Fed Variable Speed Wind Turbines", *Proceedings of NORPIE 2004*, 14-16 June 2004, Trondheim, Norway, (CD-ROM), 8 p., Available: http://www.elkraft.ntnu.no/norpie/10956873/Final%20Papers/033%20-%20Norpie_033.pdf (10.5.2006).

Holdsworth, L., Wu, X.G., Ekanayake, J.B., Jenkins, N., 2003a. "Comparison of Fixed Speed and Doubly Fed Induction Wind Turbines during Power System Disturbances", *IEE Proceedings - Generation, Transmission and Distribution*, Vol. 150, No. 3, May 2003, pp. 343-352.

Holdsworth, L., Wu, X.G., Ekanayake, J.B., Jenkins, N., 2003b. "Direct Solution Method for Initialising Doubly-Fed Induction Wind Turbines in Power System Dynamic Models", *IEE Proceedings - Generation, Transmission and Distribution*, Vol. 150, No. 3, May 2003, pp. 334-342.

Hughes, F.M., Anaya-Lara, O., Jenkins, N., Strbac, G. 2005. "Control of DFIG-Based Wind Generation for Power Network Support", *IEEE Transactions on Power Systems*, Vol. 20, Issue 4, Nov. 2005, pp. 1958-1966.

Iov, F., Blaabjerg, F., Hansen, A.D. 2003. "Analysis of a Variable-Speed Wind Energy Conversion Scheme with Doubly Fed Induction Generator", *International Journal in Electronics*, Taylor & Francis Ltd, Vol. 90, No. 11-12, 2003, pp. 779-794.

Iov, F., Hansen, A.D., Sørensen, P., Blaabjerg, F. 2004. "Wind Turbine Blockset in Matlab/Simulink General Overview and Description of the Models", Report, Aalborg University 2004, ISBN 87-89179-46-3.

Herbert, J.G.M., Iniyan, S., Sreevalsan, E. and Rajapandian, S. 2005. "A Review of Wind Energy Technologies", *Renewable and Sustainable Energy Reviews*, In Press, Corrected Proof, 29 p., Available: http://www.sciencedirect.com (4.11.2005).

Kana, C.L., Thamodharan, M., Wolf, A. 2001. "System Management of a Wind-Energy Converter", *IEEE Transactions on Power Electronics*, Vol. 16, Issue 3, May 2001, pp. 375-381.

Kanerva, S., Seman, S., Arkkio, A. 2003. "Simulation of Electric Drive Systems with Coupled Finite Element Analysis and System Simulator", *Proceedings of 10th European Conference on Power Electronics and Applications*. Toulouse, France, 2-4 September 2003, 9 p., (CD-ROM).

Kanerva, S. 2005. "Simulation of Electrical Machines, Circuits and Control Systems Using Finite Element Method and System Simulator", Doctoral dissertation, TKK Dissertations 2, Espoo, 2005, Available http://lib.tkk.fi/Diss/2005/isbn9512276100/ (7.5.2006).

Koessler, R.J., Pillutla, S., Trinh, L.H., Dickmander, D.L. 2003. "Integration of Large Wind Farms into Utility Grids Pt. I - Modeling of DFIG", *IEEE Power Engineering Society General Meeting, 2003*, Vol. 3, 13-17 July 2003, p. 8.

Kovács, K.P. and Rácz, I. (1959). “Transiente Vorgänge in Wechslstrommaschinen, Band I. Verlag der Ungarischen Akademie der Wissenschaften, Budapest, Hungary, 1959.

Krause, P.C., Wasynczuk, O., Sudhoff A.D. 1995. “Analysis of Electric Machinery”, IEEE Press, 1995, 564 p.

Ledesma, P., Usaola, J. 2001. “Minimum Voltage Protections in Variable Speed Wind Farms”, *Proceedings IEEE Porto Power Tech 2001*, Vol. 4, 10-13 Sept. 2001, 6 p.

Ledesma, P. and Usaola, J. 2004. “Effect of Neglecting Stator Transients in Doubly Fed Induction Generator Models”, *IEEE Transactions on Energy Conversion*, Vol. 19, Issue 2, June 2004, pp. 459-461.

Ledesma, P. and Usaola, J. 2005. “Doubly Fed Induction Generator Model for Transient Stability Analysis”, *IEEE Transactions on Energy Conversion*, Vol. 20, Issue 2, June 2005, pp. 388-397.

Lei, Y., Mullane, A., Lightbody, G., Yacamini, R. 2006. “Modeling of the Wind Turbine with a Doubly Fed Induction Generator for Grid Integration Studies”, *IEEE Transactions on Energy Conversion*, Vol. 21, Issue 1, March 2006, pp. 257-264.

Lund, T., Eak, J., Uski, S., Perdana, A. 2005. “Dynamic Fault Simulation of Wind Turbines Using Commercial Simulation Tools”, *Proceedings of Fifth International Workshop on Large-Scale Integration of Wind Power and Transmission Networks for Offshore Wind Farms*, April 7-8, 2005, Glasgow, Scotland, pp. 238-246.

Morren, J., de Haan, S.W.H., Bauer, P., Pierik, J.T.G., Bozelie J. 2003. “Comparison of Complete and Reduced Models of A Wind Turbine with Doubly-Fed Induction Generator”, *Proceedings of 10th European Conference on Power Electronics and Applications*. Toulouse, France, 2-4 September 2003, (CD-ROM).

Morren, J., de Haan, S.W.H. 2005. “Ridethrough of Wind Turbines with Doubly-Fed Induction Generator during A Voltage Dip”, *IEEE Transactions on Energy Conversion*, Vol. 20, Issue 2, June 2005, pp. 435-441.

Muller, S., Deicke, M., De Doncker, R.W. 2002. “Doubly Fed Induction Generator Systems for Wind Turbines”, *IEEE Industry Applications Magazine*, Vol. 8, Issue 3, May-June 2002, pp. 26-33.

Niiranen, J. 2004. “Voltage Dip Ride Through of Doubly-Fed Generator Equipped with Active Crowbar”, *Nordic Wind Power Conference*, 1-2 March 2004, Chalmers University of Technology, Göteborg, Sweden, (CD-ROM), p 7.

Niiranen, J. 2005. “Experiences on Voltage Dip Ride through Factory Testing of Synchronous and Doubly Fed Generator Drives”, *Proceedings of 11th European Conference on Power Electronics and Applications*. Dresden, Germany, 11-14 September 2005, (CD-ROM), 11 p.

Niiranen, J. 2006. “About the Active and Reactive Power Measurements in Unsymmetrical Voltage Dip Ride Through Testing”, *Nordic Wind Power Conference*, 22-23 May 2006, Espoo, Finland, (CD-ROM), p 5.

Nunes, M.V.A., Lopes, J.A.P., Zurn, H.H., Bezerra, U.H., Almeida, R.G. 2004. “Influence of the Variable-Speed Wind Generators in Transient Stability Margin of the Conventional Generators Integrated in Electrical Grids”, *IEEE Transactions on Energy Conversion*, Vol. 19, Issue 4, Dec. 2004, pp. 692-701.

Oliveira, A.M., Kou-Peng, P., Sadowski, N., de Andrade, M.S., Bastos, J.P.A. 2002. “A Non-A Priori Approach to Analyze Electrical Machines Modelled by FEM Connected to the Static Converters”, *IEEE Transactions on Magnetics*, Vol. 38, No. 2, March 2002, pp. 933-936.

Pena, R., Clare, J. C., Asher, G. M. 1996. “Doubly Fed Induction Generator Using Back-to-Back PWM Converters and its Application to Variable-Speed Wind-Energy Generation”, *IEE Proc. Electr. Power Appl*. Vol. 143, Issue 3, May 1996, pp. 231-241.

Petersson, A., Thiringer, T., Harnefors, L., Petru, T. 2005. “Modeling and Experimental Verification of Grid Interaction of a DFIG Wind Turbine”, *IEEE Transactions on Energy Conversion*, Vol. 20, Issue 4, Dec. 2005, pp. 878-886.

Piekutowski, M., Field, T., Ho, S., Martinez, A., Steel, M., Clark, S., Bola, S., Jorgensen, H.K., Obad, M. 2005. “Dynamic Performance Testing of Woolnorth Wind Farm”, *Proceedings of Fifth International Workshop on Large-Scale Integration of Wind Power and Transmission Networks for Offshore Wind Farms*, April 7-8, 2005, Glasgow, Scotland, pp. 377-386.

Pöller, M. A. 2003. “Doubly-Fed Induction Machine Models For Stability Assessment of Wind Farms”, *Proceedings of IEEE Power Tech Conference 2003*, Bologna, Italy, Vol. 3, June 23-26, 2003, pp. 6-13.

Pöllänen, R. 2003. “Converter-Flux-Based Current Control of Voltage Source PWM Rectifiers - Analysis and Implementation”, Doctoral dissertation, Acta Universitatis Lappeenrantaensis, LUT, 2003, 165 p., Available http://edu.lut.fi/LutPub/web/rikpol_diss.pdf (7.5. 2006).
Pourbeik, P., Koessler, R.J., Dickmander, D.L., Wong, W. 2003. “Integration of Large Wind Farms into Utility Grids (Part 2 - Performance Issues)”, *IEEE Power Engineering Society General Meeting,* Vol. 3, 13-17 July 2003, 6 pp.

Rodríguez, J.M., Fernandez, J.L., Beato, D., Iturbe, R., Usaola, J., Ledesma, P., Wilhelmi, J.R. 2002. “Incidence on Power System Dynamics of High Penetration of Fixed Speed and Doubly Fed Wind Energy Systems: Study of the Spanish Case”, *IEEE Transactions on Power Systems*, Vol. 17, Issue 4, Nov. 2002, pp. 1089-1095.

Runcos, F., Carlson, R., Oliveira, A. M., Kuo-Peng, P., Sadowski, N. 2004. “Performance Analysis of a Brushless Double Fed Cage Induction Generator”, *Nordic Wind Power Conference*, Chalmers University of Technology, 1-2 March, Göteborg, Sweden, Available: http://www.elteknik.chalmers.se/Publikationer/EMKE.publ/NWPC04/papers/RUNCOS.PDF (7.5.2006).

Salman, S.K., Badrzadeh, B., Penman, J. 2004. "Modelling Wind Turbine-Generators for Fault Ride-Through Studies", *39th International Universities Power Engineering Conference*, Vol. 2, 6-8 Sept. 2004, pp. 634-638.

Salman, S.K., Teo, A.L.J. 2003. "Windmill Modeling Consideration and Factors Influencing the Stability of A Grid-Connected Wind Power-Based Embedded Generator", *IEEE Transactions on Power Systems*, Vol. 18, Issue 2, May 2003, pp.793-802.

Scottish grid code SB/2. 2002. "Scottish Grid Code Panel Review", Report SB/2, Available: http://www.scottish-southern.co.uk/ssegroup/KeyDocummentsPDFs/ConsultationDoc.pdf

Singh, G.K. 2004. "Self-Excited Induction Generator Research - A Survey", *Electric Power Systems Research*, Volume 69, Issues 2-3, May 2004, pp. 107-114.

Slootweg J.G., Polinder, H., Kling, W.L. 2001. "Dynamic Modeling of a Wind Turbine with Doubly Fed Induction Generator", *IEEE Power Engineering Society Summer Meeting*, Vol. 1, pp. 644-649.

Slootweg, J.G., de Haan, S.W.H., Polinder, H., Kling, W.L. 2003. "General Model for Representing Variable Speed Wind Turbines in Power System Dynamics Simulations", *IEEE Transactions on Power Systems*, Vol. 18, Issue 1, Feb. 2003, pp. 144-151.

Stanley, H.C. 1938. "An Analysis Of The Induction Motor", *AIIE Transaction*, Vol. 57, 1938, pp. 751-755.

Takahashi, I. and Noguchi, T. 1986. "A New Quick Response and High Efficiency Control Strategy of An Induction Motor", *IEEE Transaction on Industry Applications*, Vol. IA-22, No. 5, Sept./Oct. 1986, pp. 820-827.

Tang, Y., Xu, L. 1992. "Stator Field Oriented Control of Doubly-Excited Induction Machine in Wind Power Generating System", *Proceedings of the 35th Midwest Symposium on Circuits and Systems 1992*, Vol. 2, 9-12 Aug. 1992, pp.1446-1449.

Tapia, A., Tapia, G., Ostolaza, J.X., Saenz, J.R. 2003. "Modeling and Control of a Wind Turbine Driven Doubly Fed Induction Generator", *IEEE Transactions on Energy Conversion*, Vol. 18, Issue 2, June 2003, pp. 194-204.

Thiringer, T., Luomi, J. 2001. "Comparison of Reduced-Order Dynamic Models of Induction Machines", *IEEE Transactions on Power Systems*, Vol. 16, Issue 1, Feb. 2001, pp. 119-126.

Thiringer, T., Petersson, A., Petru, T. 2003. "Grid Disturbance Response of Wind Turbines Equipped with Induction Generator and Doubly-Fed Induction Generator", *IEEE Power Engineering Society General Meeting*, Vol. 3, 13-17 July 2003, pp. 1542-1547.

Vas, P. 1992. "Electrical Machines and Drives - A Space Vector Theory Approach", Oxford University Press, New York, 1992. 808 p.

Vicatos M.S., and Tegopoulos, J.A. 1991. "Transient State Analysis Of A Doubly-Fed Induction Generator Under Three Phase Short Circuit", *IEEE Trans. Energy Conversion*, Vol. 6, March 1991, pp. 62-68.

Virtanen, R. 2004. "Configuration and Method for Protecting Converter Means", International patent application WO2004/091085, Oct. 21, 2004. Available: http://ofi.epoline.org (10.5.2006).

Xiang, D., Ran, L., Tavner, P.J., Bumby, J.R. 2004. "Control of a Doubly-fed Induction Generator to Ride-through a Grid Fault", *Proceedings of ICEM 2004*, Cracow, Poland, 5-8 September 2004, (CD-ROM), 6 p.

Yamamoto, M., Motoyoshi, O. 1991. "Active And Reactive Power Control for Doubly-Fed Wound Rotor Induction Generator", *IEEE Transactions on Power Electronics*, Vol. 6, Issue 4, Oct. 1991, pp. 624-629.

Zhang, L., Watthanasarn, C., Shepherd, W. 1997. "Application of A Matrix Converter for the Power Control of a Variable-Speed Wind-Turbine Driving a Doubly-Fed Induction Generator", *23rd International Conference on Industrial Electronics, Control and Instrumentation IECON 97*, Vol. 2, 9-14 Nov. 1997, pp. 906-911.

ISBN-13 978-951-22-8422-1
ISBN-10 951-22-8422-7
ISBN-13 978-951-22-8423-8 (PDF)
ISBN-10 951-22-8423-5 (PDF)
ISSN 1795-2239
ISSN 1795-4584 (PDF)